AN INVESTIGATION OF THE SEISMIC WAVE PROPAGATION PROPERTIES OF A THIN UNSATURATED LAYER AS A WAVE GUIDE

Thesis for the Degree of M. S.

MICHIGAN STATE UNIVERSITY
RAYMOND C. TODD

1971

AN INVESTIGATION OF THE SEISMIC WAVE PROPAGATION PROPERTIES OF A THIN UNSATURATED LAYER AS A WAVE GUIDE

By

Raymond C. Todd

A THESIS

Submitted to
Michigan State University
in partial fulfillment of the requirements
for the degree of

MASTER OF SCIENCE

Department of Geology

1971

ACKNOWLEDGMENTS

I could not list the names of all the people who have helped in the preparation of this thesis, with assistance, advice, encouragement, or information. I can only name a few men to whom I owe the deepest gratitude.

Dr. Hugh F. Bennett was my major professor and chairman of the guidance committee. Of all that is implicit in that role, I mention in particular his patience. Dr. William J. Hinze and Dr. Robert Ehrlich served on my guidance committee and gave encouragement and active assistance. Dr. Donald G. Hill, then a doctoral candidate, wrote computer programs and organized the handling of the digitised data. Richard Brown, Timothy Heenan, Innaiah Pothacamury, and Leland Younker helped in the data collection.

The Michigan State University Computer Laboratory provided computer facilities. I am indebted to the Geology Department for its support of the computer work.

I was financially assisted by a grant for research from the Office of Water Resources Research of the United States Department of the Interior.

TABLE OF CONTENTS

LIST OF TABLES

LIST OF FIGURES

CHAPTER I

INTRODUCTION

The purpose of this study is to investigate the application of some methods of earthquake seismology to seismic exploration of near-surface sediments. Since the theory of seismology can be applied to both large and small scale features, methods developed for study in one area can be applied to the study of the other. Earthquake seismology is the study of the elastic parameters and structure of the earth from observation of the propagation of earthquake derived earth motions. Exploration seismology is the study of near surface materials, mainly sediments, by seismic means using artificially induced earth motions, as from explosions.

Earthquake seismology is so called because earthquakes are the only sources of energy strong enough to produce detectable vibrations at the great distances required to provide information about very deep portions of the earth. The closely related subject of seismic crustal studies is distinguished by its more limited area of

interest--the crust of the earth--and its use of large explosions, including nuclear blasts, as energy sources in addition to earthquakes.

Exploration seismology owes its name to the fact that its methods are used in the exploration for economic resources. Geologic information from this source is responsible for the discovery of much of the world's petroleum. Exploration seismology is also used in the search for minerals, highway engineering, groundwater development, and many other fields.

Although exploration seismology employs the two basic tools of earthquake and crustal seismology, reflection and refraction, it does not make nearly as complete use of the available data as do the other fields of seismology. Of the two kinds of body waves which are known to occur in the earth, only one, the compressional wave, is used in exploration seismology. Earthquake seismology makes good use of compressional waves, shear waves, which are the second body wave, and also surface waves to obtain information which could not be obtained from analysis of compressional wave characteristics alone.

The petroleum industry, by far the largest user of seismic methods, does not make use of the information which could be obtained from non-compressional waves. Almost invariably, the arrivals of surface and shear waves are considered as "noise" on the records. These waves do contain information, and attempts to make use of this data

are found in numerous papers in the seismic literature. For example, Dobrin (1951, 1954), Jolly (1956), and White (1956, 1964) have reported on field studies involving non-compressional waves.

Possibly one reason why these experimental attempts to use multi-component recording have not been more successful is that wave motion in each of the component directions has usually been evaluated separately from the others. The report by Shimshoni (1964) is an example of a recent trend toward analyzing the data from two or more components together to produce an output combining data from each of the components.

Since the various waves are distinguished by the direction of their particle displacement, they can in principle be recognized from the records of a three-component recording system. Except under ideal conditions, however, it is difficult or perhaps impossible to recognize some wave arrivals simply by inspection of the records. This investigation is an attempt to enhance the wave arrivals by data-processing manipulations of the recorded signals. Success in recognizing arrivals of non-compressional waves would indicate that more information can be obtained by using three-component geophones and computer processing of the resulting three-component data than can be obtained with the usual single-component recording.

This study was designed to test the feasibility of identifying some of these later arrivals in a reasonably simple geologic situation. The area chosen for the field work is a good approximation to the three-layer seismic refraction model. The surface layer is an unsaturated sandy till with compressional velocity of about 1150 feet per second. Underlying this is water-saturated till which has a compressional velocity of about 5700 feet per second. The third layer is the bedrock with velocity of about 12,500 feet per second. The depth to the water table, which is the interface between the first and second layers, ranges from 5 to 30 feet, depending on location. The depth to the bedrock is approximately 500 feet.

The geologic setting is described more fully in the following chapter.

CHAPTER II

LOCATION AND GEOLOGY OF THE FIELD AREA

The field area was chosen for its simple geology, well-known water table depths, and flat topography. It is located in the Udell Experimental Forest, a part of the Manistee National Forest, Manistee County, Michigan. Figure 1 shows the location of the field area and the three sites where the seismic work was conducted.

This area is part of a glaciated region whose topography consists primarily of outwash plains and morainal features. The field area itself is flat and level, but only a few miles away is the prominent feature known as the Udell Hills, from which the area takes its name. The Udell Hills are a circular mound of drift which rises 300 feet above the surrounding area and is about three miles in diameter. It is interpreted as a morainal feature. Its edges appear to have been fluvially dissected with resultant rough topography (U.S. Geological Survey, 1957).

Logs of oil wells near the field area show that the glacial deposits are floored by Mississippian strata--the Coldwater Shale, the Marshall Sandstone, and the Michigan

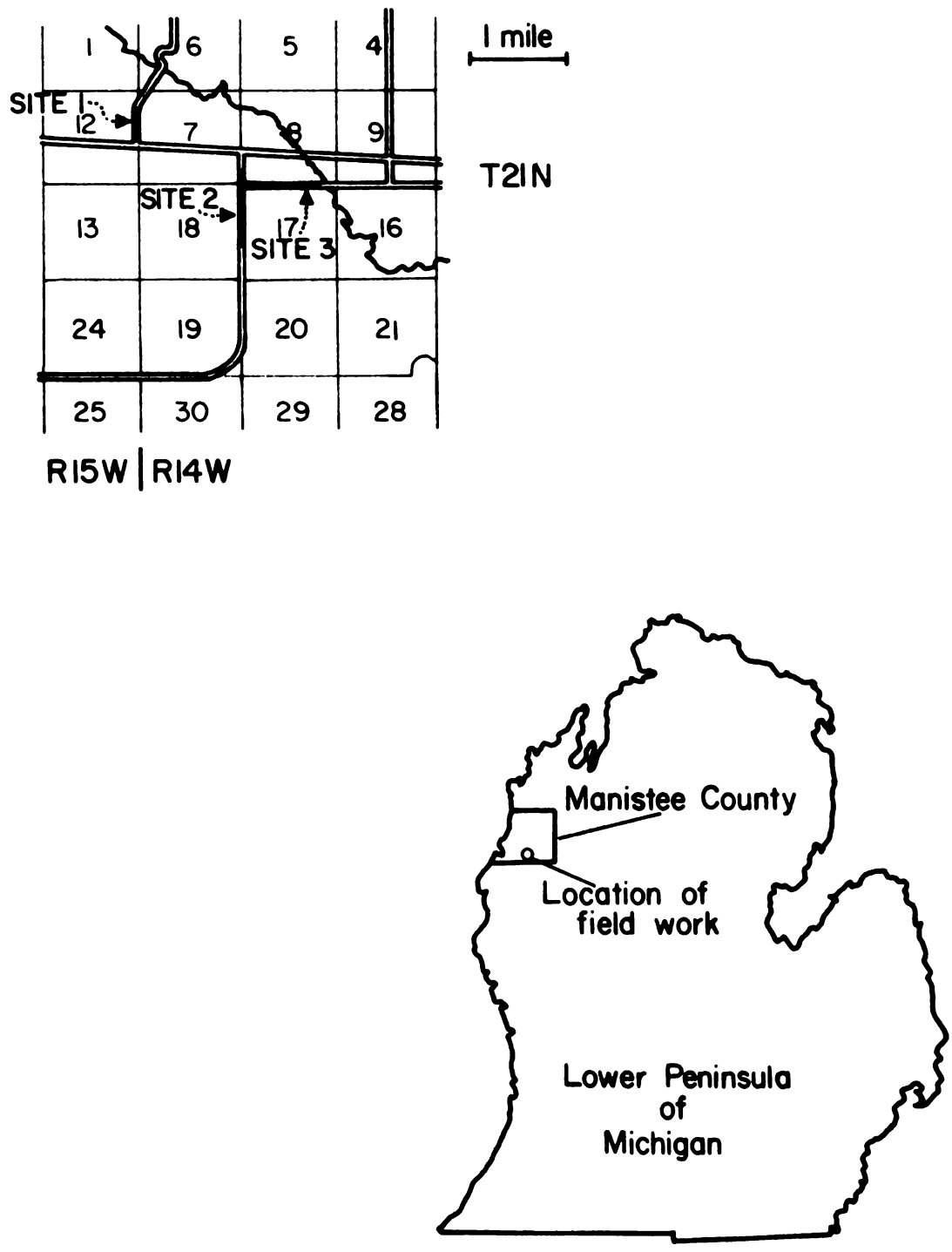

Figure 1.--Location of field sites.

Formation. The Michigan Formation is most frequently reported. Because none of the wells are closer than four miles to the field area, it is difficult to predict which of these units underlies the field area. The following is a summary of the available information about the three formations, which are not described in detail in these logs. The Coldwater shale, the oldest of the three, is a shale which contains small amounts of limestone and sandstone. It is mostly gray and is about 500 feet thick. Above this unit is the Marshall Sandstone, a sandstone about 200 feet thick and with small to considerable quantities of shale. Finally, the Michigan Formation, the youngest, was only reported once, as 20 feet of blue shale. However, the available logs are basically driller's logs and were not originally prepared by geologists. For this reason they cannot be relied upon for complete accuracy.

The overlying glacial drift is of Pleistocene age. The well logs indicate that the drift is principally sand with some clay layers in varying proportions. In general, the amount of clay is small compared to the sand. The surface material is a moderately clean sand. The seismic results suggest that the drift contains no significant amounts of clay at the sites of the seismic investigations.

A portion of the geologic column in the field area is shown in Figure 2. The Paleozoic rocks shown were

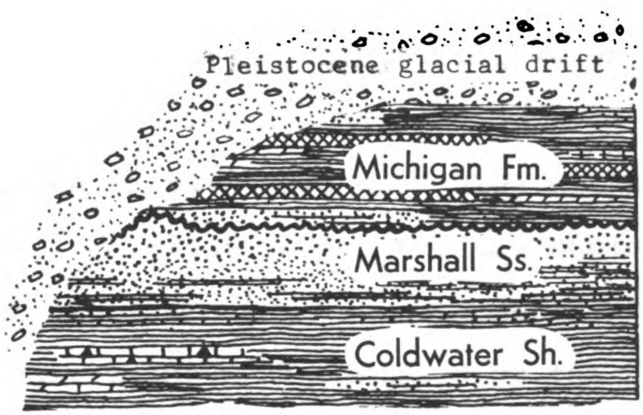

Pleistocene	Quaternary
Mississippian	Paleozoic

Figure 2.--Portion of stratigraphic section in Michigan.

taken directly from the stratigraphic column published by the Michigan State Geological Survey (1964).

The available data from well logs on the bedrock and drift thickness are shown in Figure 3. For each well, the formation present at the bedrock surface is indicated by a symbol, and the thickness of the drift is given. The indicated drift thicknesses range from 200 to 600 feet, but are subject to the limitation on the reliability of drillers' logs. The seismic data show that the bedrock depth in the field area lies within this range.

A major reason for the choice of this area is that the depth to the water table is well-known from a series of observation wells drilled by the U.S. Forest Service. In addition, the water table was sometimes reached in drilling shallow holes for the placement of explosives. The depth of the water table ranges from 5 to 32 feet under the sites used in this investigation.

The field area thus consists of permeable unconsolidated sediments overlying less permeable sedimentary rock. The unconsolidated detritus is only partially saturated and therefore has a well-defined water table. The physical characteristics of the area thus provide three nearly horizontal interfaces: the topographic surface, the water table, and the contact of the Mississippian bedrock with the Pleistocene glacial drift. This thesis is basically a study of the effects of these interfaces on some seismic waves.

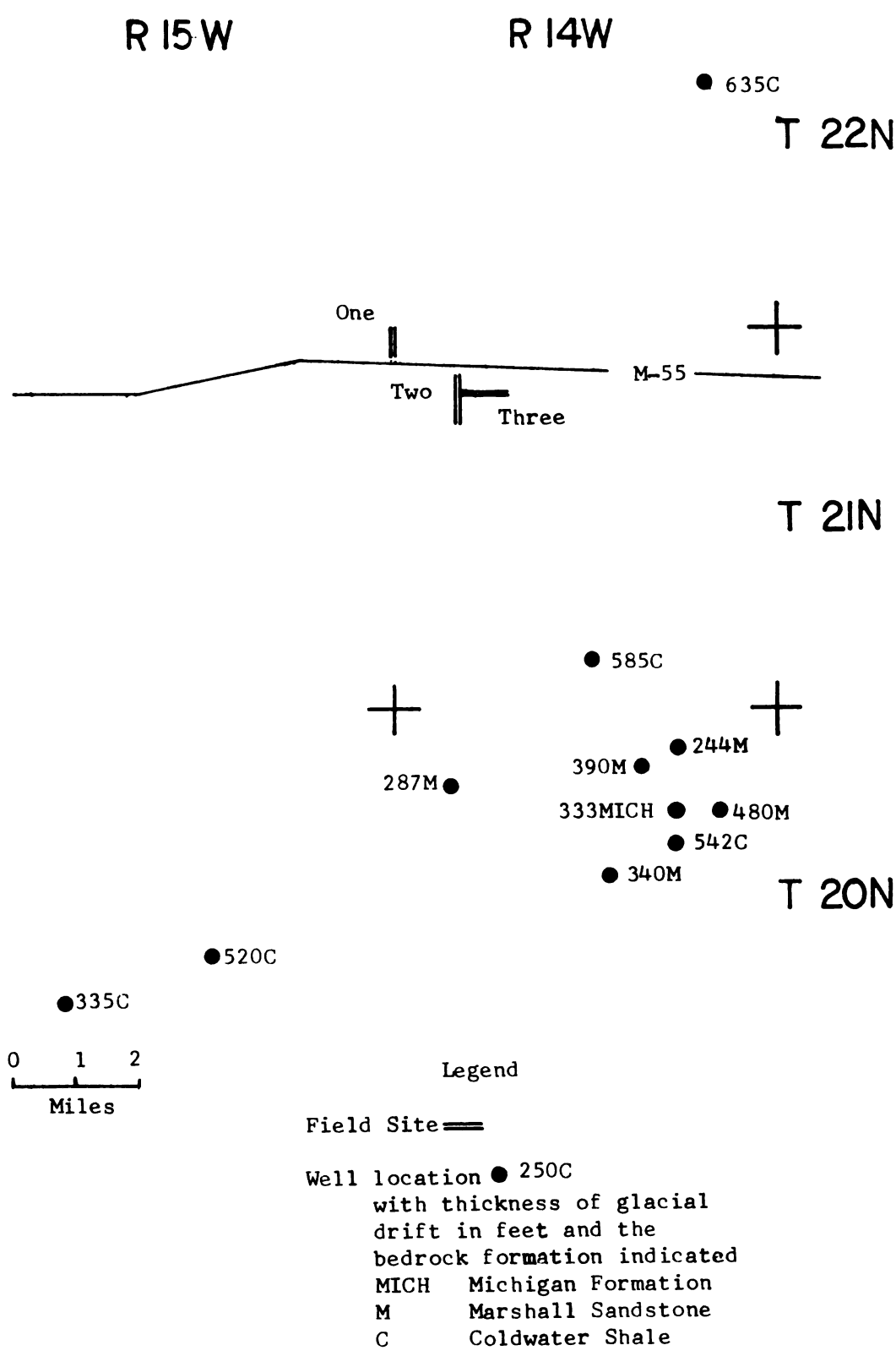

Figure 3.--Depth to bedrock and bedrock formation from well log data.

CHAPTER III

DATA COLLECTION

Field Equipment

Introduction

The purpose of the field work was to record earth vibrations which had been generated at some distance from the recording point. The nature of the received earth vibrations and their arrival time were used in accordance with the principles of seismology to obtain information about the earth materials through which they have passed. The seismic signals were generated mostly by the detonation of small explosive charges buried in the earth. The seismic signals were detected by geophones of the moving coil type, which generate an electrical signal in response to earth movements. A seismic recording unit recorded the electrical signals on photographic paper.

Geophones

Eight three-component geophones were used to record the seismic signals. Each geophone was actually three

geophones in one instrument case, with each geophone sensitive to motion in one of the three component directions. It is characteristic of moving coil geophones that the voltage response at any one frequency is proportional to the velocity of ground movement, at least for movements with frequency higher than the natural frequency of the geophone. The natural frequency of the geophones used is 4.5 hertz, which is much lower than that of the seismic signals of interest in this investigation. The damping was 62% of critical, and the geophone response was linear at frequencies higher than 7 hertz, according to the response curves published by the manufacturer (Geo Space Corporation, 1965).

Because particle motion is described by theoretical seismology in terms of particle displacement, it would have been more desirable to have recorded the ground motion in terms of particle displacement. The particle velocity which was recorded is the time derivative of the displacement. However, because seismic displacement functions usually have a sinusoidal appearance, the velocity function also exhibits this characteristic.

As a result, the amplitudes of high frequency waves appear higher than those of low frequency waves, relative to original signals with the same displacement amplitude. This occurs because the higher frequency signals have a greater rate of change with time than the lower frequency signals. This distortion can be accepted because it tends to enhance

the usually relatively weak high frequency portions of the original seismic signal. Thus it is less likely that information contained in these higher frequencies will be lost. Also, the energy carried by an elastic wave is proportional to the square of the velocity amplitude but has no simple relation to the displacement amplitude.

Recorder

The 24 signals from the eight geophones were recorded in an analog fashion by an exploration type seismic recording unit made by the Gulf Research and Development Company, probably in the period 1952-54. The recorder has amplifiers for each of the 24 channels, and the amplifier gain, filter setting, and automatic gain control setting can be indepentently adjusted for each channel. However, for most of the records used here, all amplifier gains were identical, and neither automatic gain control nor filtering were used. The output of each amplifier was connected to a mirror galvanometer.

The signals were recorded on the photographic paper as it passed over a bank of 24 mirror galvanometers, each of which reflected a spot of light on the paper. A stationary spot represents a zero signal and appears on the paper, after developing, as a straight line. Fluctuations in the signal cause the light spot to move, and then the displacement of each line from its zero-signal

position is a measure of the input voltage and therefore the velocity of ground movement.

During the recording process, the flashing of a light at 0.005 second intervals causes time marks to appear across the record. The timing lines are vertical in contrast to the signal lines which are horizontal. This make it possible to accurately determine the time interval between seismic events recorded on the paper. The film is developed in the conventional way for photographic papers. Figure 4 shows a portion of one of the original records. The zero time, i.e., the timebreak, is labeled along with the 0.5 second times. The geophone directions are labeled HL, V, and HT, which represent horizontal facing the shotpoint, vertical, and horizontal perpendicular to the shotpoint, respectively.

Explosions

The explosives used were nitro-carbo-nitrate charges packed into metal cans, each containing one pound. The cans had screw ends so that larger charges could be made by stacking several cans end-to-end. The explosive was detonated by an electric blasting cap inserted into a hole in the top can, which contained a primer explosive needed to detonate the relatively insensitive nitro-carbo-nitrate.

A capacitor-discharge blaster, Geo Space Corporation model HS-200, fired the blasting cap. Also, it transmitted

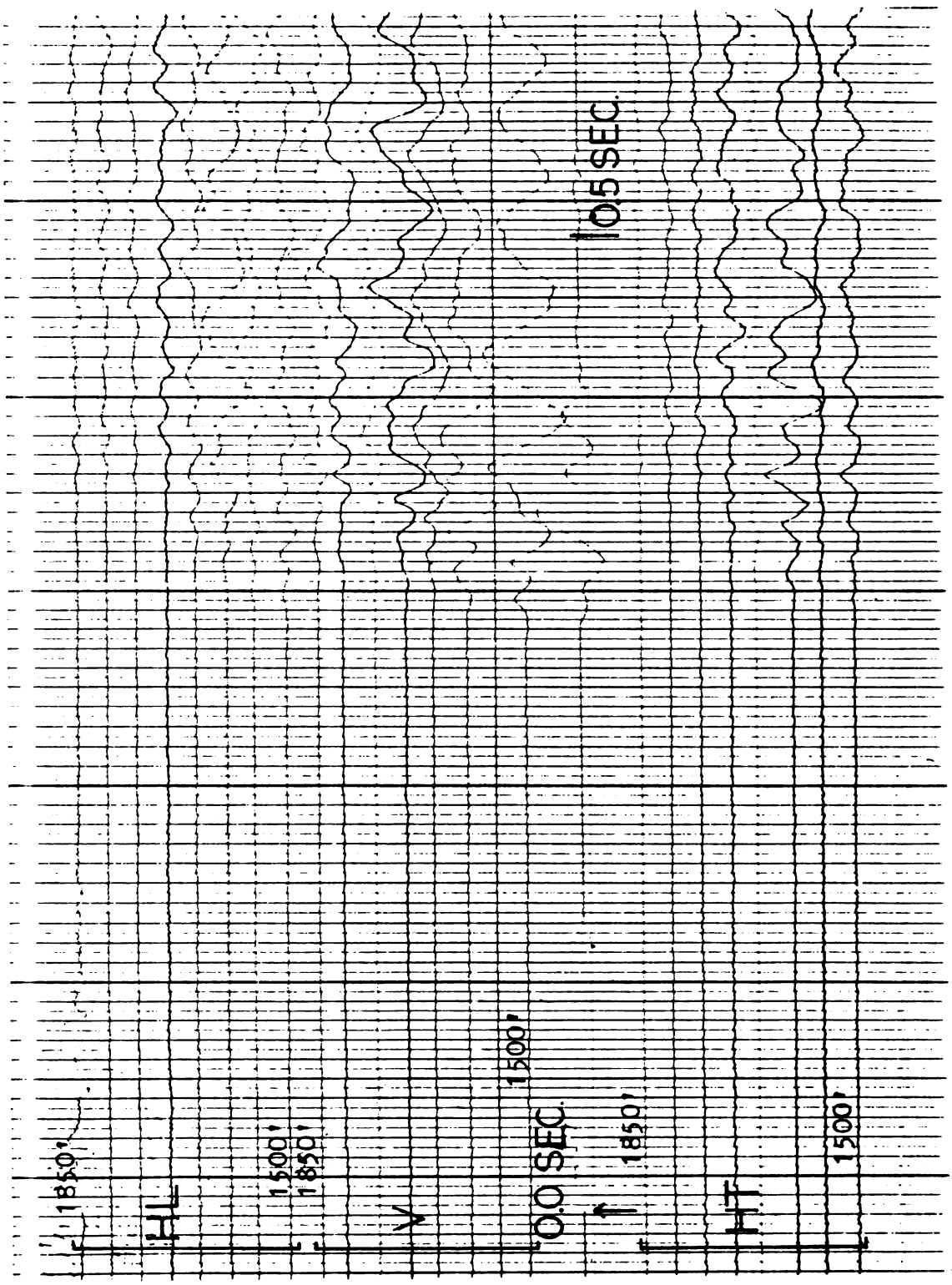

Figure 4.--Portion of an original seismogram.

a timebreak signal to the recording unit along a two-wire cable, which was also used to connect sound-powered telephones for coordinating the firing with the operation of the recording unit.

Field Procedures

Geophone Arrays

Interpretation of the seismic records requires knowledge of the distance between source and each detector and the depth of emplacement of the geophones and the explosive charge. The geophones were located in a straight line array, with a constant distance between each geophone. For Site One this was 30 feet; for Sites Two and Three it was 50 feet. The array was always parallel to a road so that the shot points could easily be located in line with the geophone array.

The geophones were buried in a vertical position just below the surface. Soil was tamped around them to provide as good coupling with the ground as possible. The geophones were oriented so that one horizontal component geophone faced the shotpoint. Signals from this component geophone were labeled HL (Horizontal longitudinal); for the other horizontal component geophone the signals were labeled HT (Horizontal transverse); and from the vertical geophone V (Vertical).

Shotpoints

The explosive charges were buried in holes made with a soil auger. The first shotpoint was usually located so that its distance from the closest geophone was about the same as the total length of the geophone array. Four or five more shots were then fired at increasing distances from the geophone, with the separation between successive shotpoints against about the same as the geophone array length. In some cases a final shot was fired very close to the end of the array. This general procedure was used so that the records would include shotpoint-geophone distances spaced regularly over the range of minimum to maximum distances. These might be as low as 10 feet if the close shotpoint was used, to a maximum of 2350 feet.

As an example of the shooting procedure, the method used at Sites Two and Three will be described. At these sites the geophone spacing was 50 feet and the array length was 350 feet. The shotpoints were 350, 700, 1050, 1500, or 2000 feet away from the nearest geophone. For the shotpoint at 350 feet, the shotpoint-geophone distances ranged from 350 feet to 700 feet (the furthest geophone) at 50-foot intervals. The next shotpoint covered 700 to 1050 feet in the same way. The remaining three shotpoints covered the interval from 1050 to 2350 feet with a few gaps. The close-in shot, if used, was at 10 or 20 feet. Thus a series of shotpoint-geophone distances resulted over a wide range with 50-foot separation.

After firing shots on one side of the array, a similar series of shots were fired on the other side. In this way, the geophones received seismic waves that had traveled in opposite directions. As will be seen later, this is necessary to resolve ambiguities in the interpretation of refraction results in an area where the interfaces between layers are not known to be level. Figure 5 shows a portion of the physical layout for Sites Two or Three.

Hammer Blows as Energy Sources

Also in the Udell field area, hammer blows were used to measure seismic velocities over short distances, to determine the velocity at shallow depth and to study the first motions and effects of polarization. The blows were directed against a steel plate placed either on the bottom or against the sides of a small rectangular pit, a short distance from a recording array. Blows were struck in five directions, i.e., vertical and in the four horizontal directions. The most significant result was the determination of the shear velocity in the unsaturated sand. These experiments showed that it is about 600 feet per second.

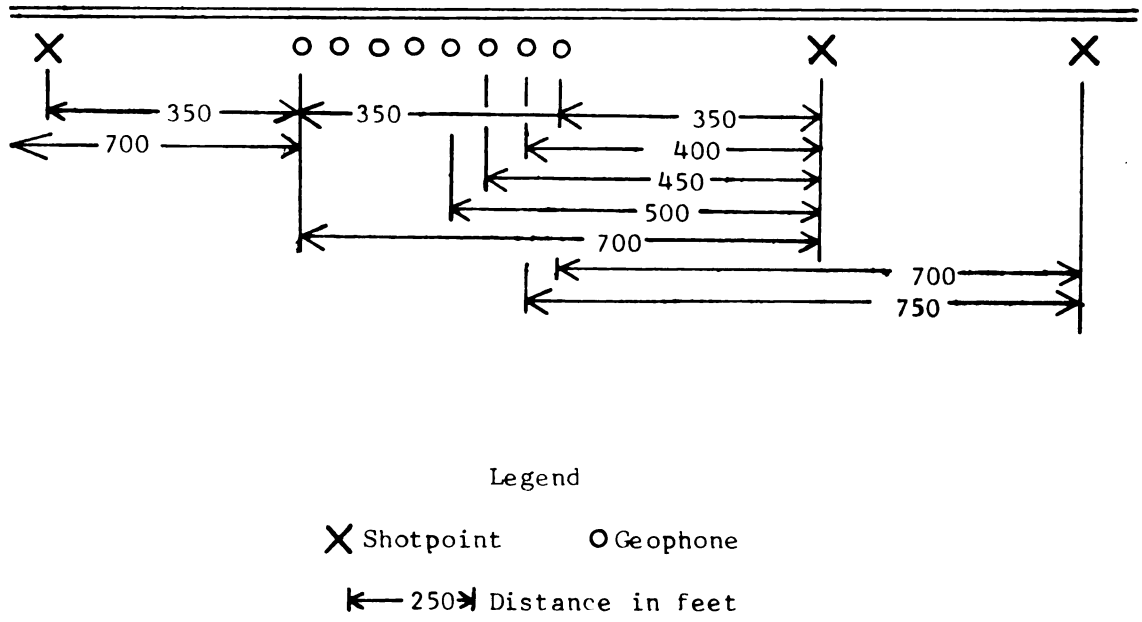

Figure 5.--Plan view of physical layout used at the seismic field sites.

CHAPTER IV

DATA PREPARATION

Digitizing

In order to process the analog data with a computer, it was necessary to obtain a numerical representation of it. This was done by digitizing the recorded traces. The digitizer used, a Pencil Follower Type PF10000, was made by D-Mac Limited, Glasgow, Scotland. The digitizer was operated by moving a transparent plastic "reading pencil" over the seismic record so that the crosshairs of the pencil follow a trace of the record.

Successive positions of the pencil were punched in digital form onto computer cards by an IBM card punch wired to the digitizer. The data was in a format of eight columns for a recorded point, with the first four giving the position along the X-axis and the second four the position along the Y-axis. The X-axis is parallel to the long direction of the table. The coordinates punched are the distances from the origin at the lower left-hand corner of the table and are in units of tenths of millimeters. In setting up the record on the reading table,

it was carefully aligned so that its time axis was parallel to the X-axis of the digitizer. Also, prior to digitizing each trace, the X-coordinate of the timebreak and the Y-coordinate of the zero signal level were recorded.

The digitizer can be operated in three distinct modes of operation. Two of them were not suited for the present study and will be mentioned only briefly. The first of these is the position mode, in which the current position of the reading pencil is recorded each time a footpedal is pressed. The X-mode records the position of the reading pencil every time the X-coordinate changes by a preset number of millimeters. The position mode would require too many manual operations of the footpedal. The X-mode would have been ideal except that under its control, a seven-column field was frequently substituted for an eight-column field with the result that all subsequent fields on the same card or later cards were one column out of place. The errors required immediate manual correction and happened so frequently that the mode was nearly useless for the purposes of this work.

The time mode, which was used, causes the coordinates of the location of the reading pencil to be punched at present time intervals. The number of points sampled per unit distance on the seismogram depends on the speed with which the pencil is moved. In general, the portions of the seismograms representing low frequencies were digitized with faster pencil movement than the more complex

higher frequency portions. In this way, a roughly similar number of points were sampled over each cycle of the signal waveform. High frequency signals were sampled as frequently as was needed to reproduce them, while the faster pencil movement over low frequency portions speeded up the digitizing work. The operation of the digitizer is described in more detail in the Appendix.

The "Playback" Program

The computer program "Playback," written by Donald C. Hill, was used to prepare a more orderly presentation of the digitized data. It corrected some digitizer errors, transformed the data so that it was given relative to zero time and zero amplitude positions, interpolated between recorded points to provide amplitude values at regularly spaced intervals, and finally changed the format of the data. It was also capable of applying a gain factor to all the points in a trace. This could be used to normalize the amplitudes of traces recorded at different gains.

The program eliminated erroneous data caused by the occasional dropping of the last three significant figures of a coordinate. For example, 124.7 millimeters might become 100.0 mm as the last three digits were replaced by zeros. When this happened to an X-value, it was easily detected because the increasing order of the X values was disturbed. However, it was much harder to find a criterion

for recognizing its occurrence to a Y-value. The criterion finally adopted was that any Y-value that differed by more than 2.0 mm from the preceding Y-value was ignored.

The remainder of the calculations were relatively straight-forward. The X-coordinate of the timebreak was subtracted from the X-values and the Y-coordinate of the zero signal amplitude was subtracted from the Y-values. Y-values were generated by interpolation at one millimeter intervals from the corrected data X-values. The format of the data was thus changed from an X, Y, X, Y, etc. alternating sequence to a sequence of Y-values, with the corresponding X-values implicit in the position of the Y-values in the sequence.

Two other calculations of lesser importance were performed. One was the application of a scale factor to all the corrected Y-values, so that channels recorded at unequal gains could be normalized. The second changed the X-values on input to compensate for slight differences from one record to another in the distance between timing marks, i.e., the ratio between time and X-distance. The difference from one record to another was rarely over 1 per cent.

Following the computations and corrections, two representations of the new seismogram were included in the program output. The seismogram was drawn by the computer on a Calcomp digital plotter so that the fidelity of the

digitization and subsequent processing could be checked by comparison with the original record. The corrected Y-values were also punched onto a new deck of computer cards. This deck contained the original data in a form which is much more suitable for computer processing. A flow chart of a portion of the Playback program is shown in Figure 6. The program, its input deck, and its output deck are further described in the Appendix.

The Absolute Signal Magnitude Presentation

A method of combining the data representing the particle velocity in each of the three component directions was sought to provide a practical means of distinguishing different types of wave motion. The method used in this study was the preparation of plots showing the magnitude of the resultant vector of the three components as a function of time without reference to the direction of the resultant vector. The resulting presentation is given the name absolute signal magnitude. It could have been called an absolute particle velocity magnitude presentation, but the word "signal" is used because the starting point is the voltage output or signal from the geophones.

The absolute signal magnitude plots were calculated from the corrected data generated by the playback program. If we let x, y, and z be the particle velocities in the three component directions at a point in time, the absolute signal magnitude at that time is calculated as

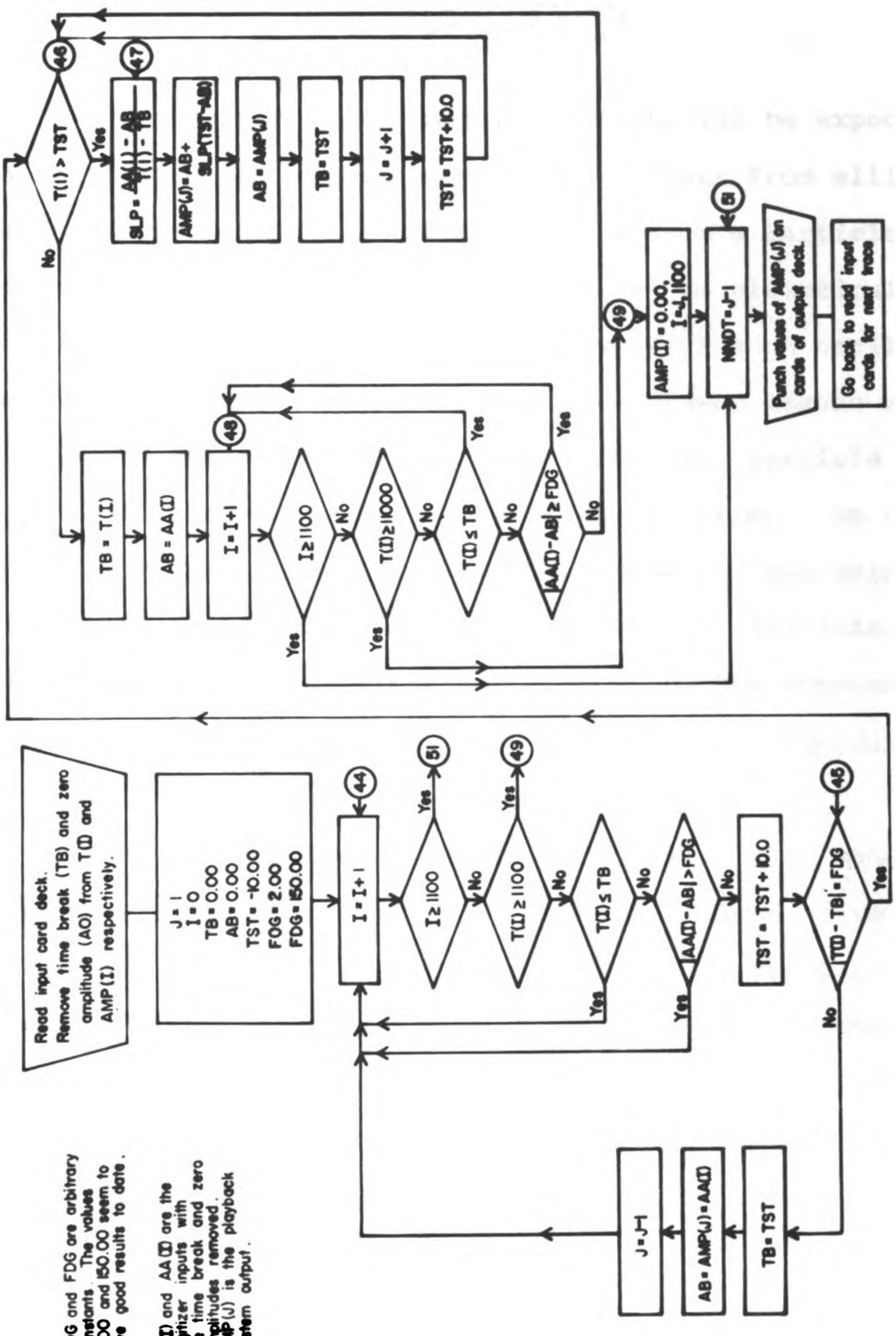

Figure 6.--Flow chart of Playback processes.

$$a = \sqrt{x^2 + y^2 + x^2}$$

The absolute signal magnitude plots can be expected to facilitate the distinction of rectilinear from elliptical particle motion. In rectilinear motion a particle moves back and forth in a straight line; in elliptical motion a particle describes an ellipse with each oscillation. The absolute signal magnitude cannot become zero during the passage of a wave with elliptical particle motion because the particle is always in motion. In contrast, the absolute signal magnitude becomes zero twice during each cycle of a wave with rectilinear particle motion. Figure 7 illustrates the relationship between rectilinear and elliptical particle motion and the corresponding absolute signal magnitude plots.

The calculations resulting in the absolute signal magnitude plots were made by a computer program called SMOV, also written by Donald G. Hill. The plots were again made with a Calcomp plotter under computer control. Program SMOV, along with the Playback program, is listed in the Appendix. The order and significance of the cards in the input and output decks are also described.

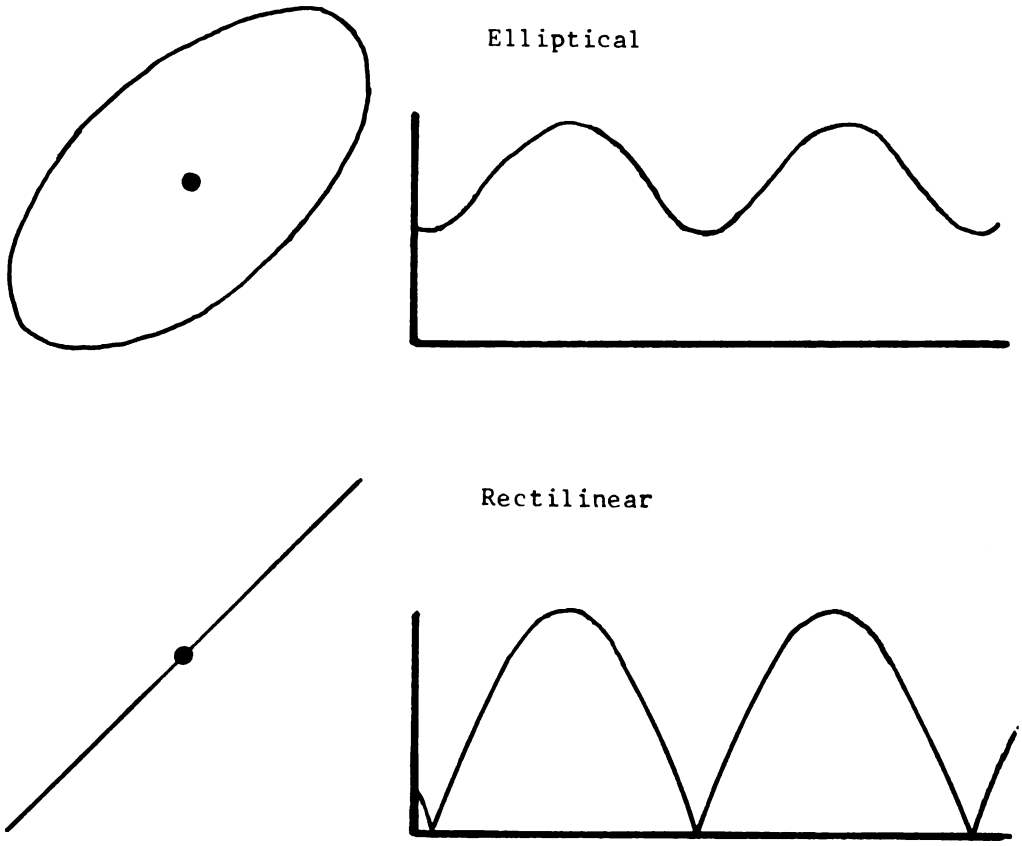

Figure 7.--Comparison of the absolute signal magnitude plots resulting from elliptical and rectilinear motion.

CHAPTER V

TRAVEL OF SEISMIC WAVES

Introduction

A sizable number of distinct seismic waves exist. The most basic distinction among them is that between body and surface waves. Surface waves effectively are limited to traveling along a boundary, as their amplitude decreases exponentially with depth. Body waves can travel through all portions of a solid. Different patterns of particle motion form the basis for identification of individual wave types.

The following discussion will be based on the assumption that the material is isotropic, that it is homogeneous, and that it is perfectly elastic. All physical properties of an isotropic material are identical regardless of the direction in which they are measured. A homogeneous material has the same properties at all points. For example, sheets of paper stacked together are homogeneous but not isotropic. But the stack is homogeneous only on a gross scale; on a small scale it would be considered to consist of two materials, paper and air, the

latter trapped between the sheets. Finally, a substance is perfectly elastic if its distortion in response to an applied force is always exactly proportional to that force.

There are only two types of body waves: compressional and shear waves. They both have rectilinear particle motion. When the particle motion is parallel to the direction of propagation, the wave is a compressional wave. It may also be called a longitudinal or a "P" wave. A shear wave's particle motion can be in any direction that is perpendicular to the propagation direction, but two special cases have been given names. An SH wave is a shear wave with horizontal particle motion, and an SV wave is one whose particle motion lies in the incident plane--the vertical plane containing the wave path.

A large number of surface waves exist. Only two, the Rayleigh and the Love waves, are reported with any frequency in the literature of seismic field studies. Particles disturbed by a Rayleigh wave move in a retrograde ellipse around their original position. The ellipse is higher than it is wide and is in the incident plane. The Love wave can exist only in a relatively thin surface layer of low shear velocity material lying over material of greater shear wave velocity. It is the sum of a number of horizontally polarized shear (SH) waves, each of which takes a slightly different path from the others and is multiply reflected from the upper and lower boundaries of

the surface layer. As will be seen later, the direct compressional arrival in this study is the first of a family of arrivals which is somewhat analogous to the Love wave because of the multiple reflection of compressional waves within the surface layer.

Equations of Wave Motion

The transmission of compressional and shear waves in an elastic material is described by the following differential equations:

Compressional wave:

$$\frac{\partial^2}{\partial t^2}\left[\text{div } \vec{D}\right] = V_p^2 \nabla^2 \left[\text{div } \vec{D}\right]$$

Shear wave:

$$\frac{\partial^2}{\partial t^2}\left[\text{curl } \vec{D}\right] = V_s^2 \nabla^2 \left[\text{curl } \vec{D}\right]$$

The vector $\vec{D}$ is the displacement vector of an individual particle. The notations of vector calculus used in these equations will be explained after defining some symbols. Let u, v, and w be the x, y, and z displacements, respectively. Then curl $\vec{D} = (\theta_x, \theta_y, \theta_z)$ where

$\theta_x = \left(\frac{\partial w}{\partial u} - \frac{\partial v}{\partial z}\right)$, $\theta_y = \left(\frac{\partial u}{\partial z} - \frac{\partial w}{\partial x}\right)$, and $\theta_z = \left(\frac{\partial v}{\partial x} - \frac{\partial u}{\partial u}\right)$.

Also, div $\vec{D} = \frac{\partial u}{\partial x} + \frac{\partial v}{\partial u} + \frac{\partial w}{\partial z}$.

The phase velocities of the two waves appear in the equations as V_p and V_s, respectively. In terms of fundamental constants, they are

$$V_p = \sqrt{\frac{k + 4/3\ \mu}{\rho}}$$

$$V_s = \sqrt{\frac{\mu}{\rho}}$$

where:

k = bulk modulus or compressibility

μ = shear modulus

ρ = density.

Unfortunately, no similar equations can be given for the surface waves. The velocity of the Rayleigh wave is commonly stated as 0.92 V_s (Richter, 1958, p. 241). The Love wave, because of its dispersive nature must also be somewhat slower than the shear velocity. In most solids, the physical properties are related in such a way that the shear velocity is about half of the compressional velocity, but this is not a hard and fast rule.

Wave Travel Paths

Seismic waves arriving at a given point from a source may have traveled along a number of paths. The simplest of these is the direct path, a straight line from source to detector, but the wave may also be reflected or refracted at the interfaces joining different

earth materials. Because the path taken determines the travel time, the arrival times are very useful in finding out which path a wave has taken. Usually, a plot is made of the arrival times versus the distance from source to the detector or detectors.

Figure 8 shows a time distance plot for a three-layer case. There are three earth materials present. Each has a characteristic velocity, and these velocities are distinct from one another. The surface material has the lowest velocity and the deep material has the highest. It is assumed that the surface and all interfaces between one material and another are horizontal. The lines shown connect corresponding arrival times plotted for detectors on either side of the source, which is at the surface at S. As shown in the figure, the velocities of respective materials are v_0, v_1, and v_2. Layer thicknesses are d_1 and d_2.

The curves on the time-distance plot are labeled. Line (1) represents the direct path along the surface. Accordingly, the wave travels at V_o, and the slope of this line is $1/V_o$. Line (2) shows arrival times for the wave refracted along the top of the V_1 layer; its slope is $1/V_1$. Refracted waves cannot arrive at the surface any closer than the critical reflection, shown by an asterisk. Curve (3) in tangent to line (2) at this point. Curve (3) shows the arrival times for a wave which has traveled down to the V_1 material and has been reflected

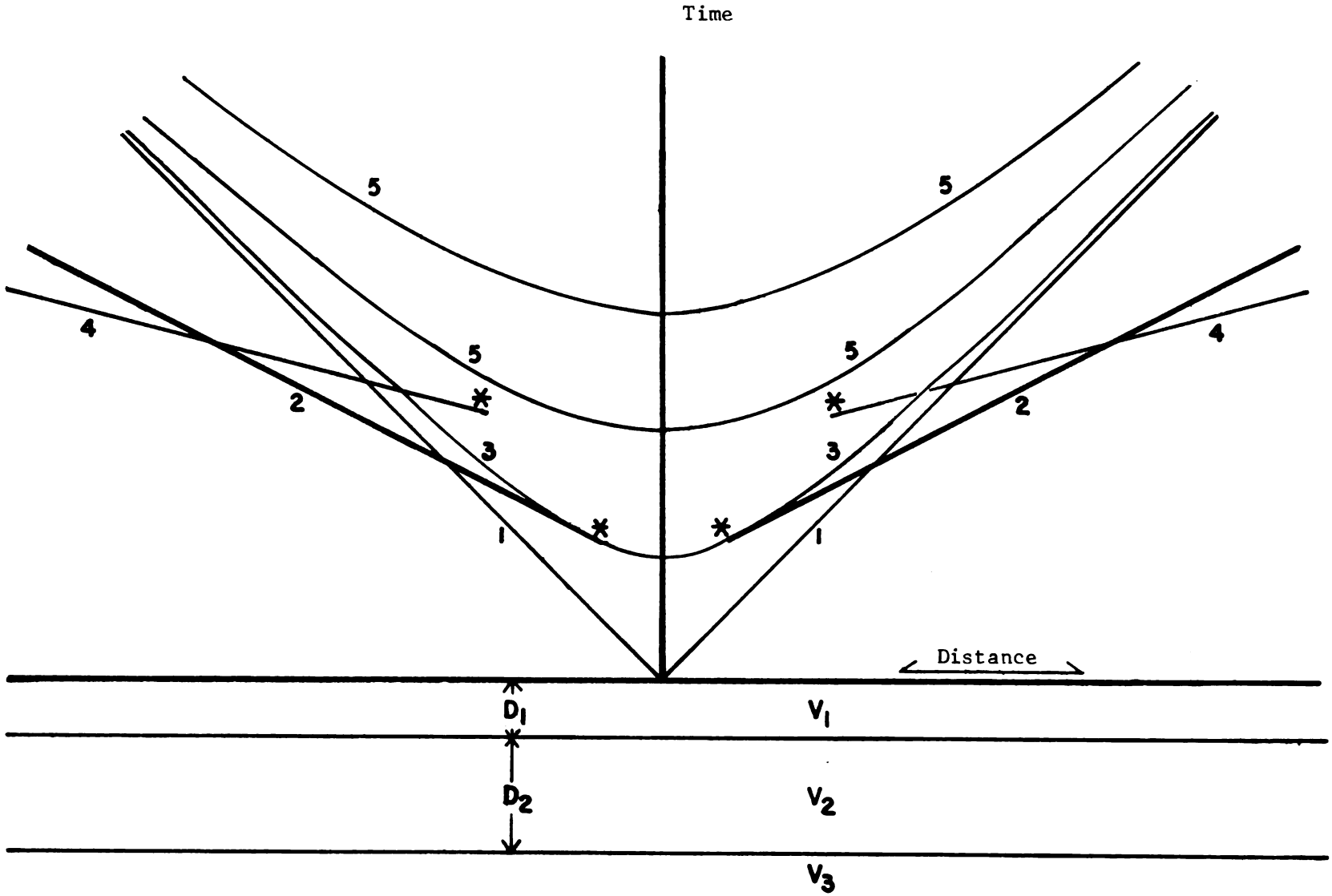

Figure 8.--Generalized time-distance plot for a three layer case.

back up. The critical reflection is common to both curves (2) and (3) because it is a reflection at the critical angle, which is characteristic of the refracted wave paths.

Line (4) is the travel time for waves which have been transmitted through the V_1 material and then critically refracted on reaching the V_2 material, so that the waves travel along the top of the V_2 layer as predicted by seismic ray theory. The critical reflection is again shown by an asterisk, although for simplicity no other reflections are shown.

Curves (5) are multiple reflections from the V_1 material. The first of these is really curve (3). All of these curves represent travel paths entirely in the V_0 material with reflections from the surface and the V_0 - V_1 interface.

Wave paths with many more reflections than those indicated here can exist. It can be seen from the asymptotic approach of the curves to line (1) that the multiple reflection times approach that of the direct path. It is to be expected that at great distances, their travel times become nearly indistinguishable from that of the direct path. The observed "direct arrival" is thus a combination of the actual direct arrival and a number of multiple reflection arrivals.

The depths to the interfaces can be calculated from the velocities and time intercepts of the time-distance

plot. If the interfaces are not horizontal, the apparent velocities from a time-distance plot are not identical with the actual velocities in the material. The apparent velocity of a wave traveling updip along an interface is greater than the actual velocity, and traveling downdip it is lower. The actual velocity and the dip angle can be calculated from a reversed time-distance plot.

Seismic waves travel at velocities determined by the physical properties of the material in which they travel. But the time taken to arrive at a given point depends on three factors: the type of wave, its velocity in the earth materials, and the geometry of the distribution of materials. From a time-distance plot of seismic arrivals, it is often possible to identify certain arrivals with a proposed ray path. With sufficient information from time-distance plots, a considerable amount of information about the earth can be deduced, including the velocities and thicknesses of each layer of earth materials.

CHAPTER VI

MODELS FROM SEISMIC REFRACTION DATA

Interpretation Principles

The field techniques used in this study are a modification of the conventional refraction method of exploration seismology. Like the conventional method, the modified method can be used to find the compressional velocities of the surface material and the velocities in one or two deeper layers, the dip of the interfaces between the layers, and the depths to the interfaces at each end of the profile. Three assumptions must be met for the calculations to be strictly valid. These are that the velocity in each material is constant throughout, that each layer has a velocity higher than that of the layer above it, and that each interface is a good approximation to a perfect plane.

The physical arrangements used to gather data in the conventional refraction method are shown in the lower part of Figure 9. A shotpoint is located at each end of the profile, and a number of geophones are spaced in between. When explosives are detonated at one shotpoint, a geophone is usually located at the unused shotpoint at the other end.

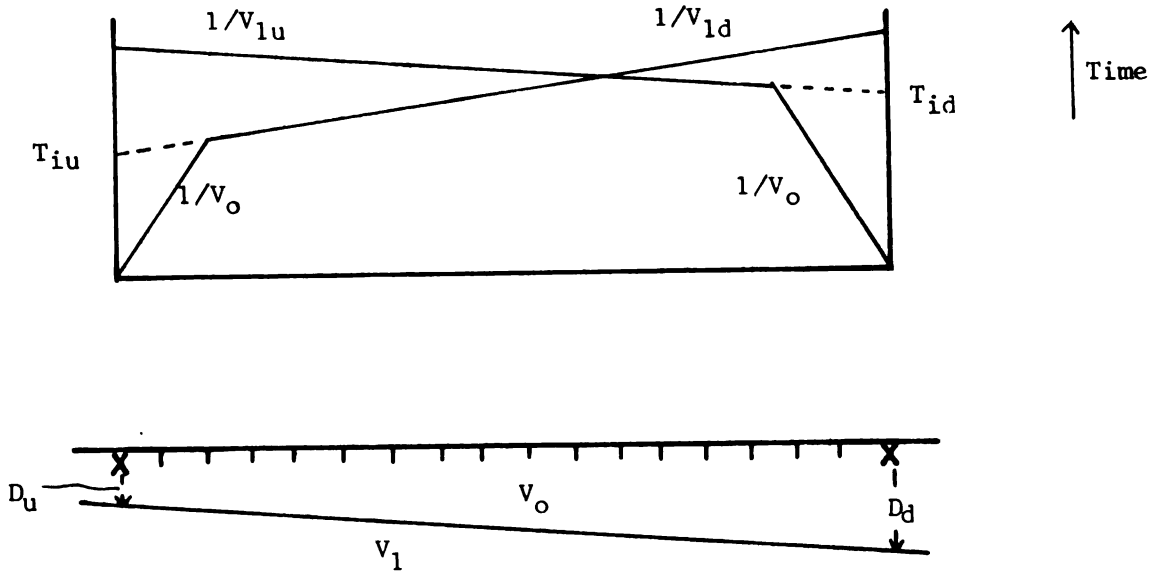

Legend:

V_o, V_1	Seismic velocities
T_{iu}, T_{id}	Intercepts of updip and downdip segments
D_u, D_d	Depths to interface at updip and downdip ends of profile
V_{1u}, V_{1d}	Apparent velocities of updip and downdip refractions from V_1 layer
X	Shotpoint
⊤	Geophone

Figure 9.--Seismic refraction over a dipping layer in the conventional method.

The parameters which can be calculated from a time distance plot resulting from the shots on each end of the profile are also indicated in the figure. These are V_0 and V_1, the velocities of the two earth materials, the depths; D_u and D_d, the depths to the interface at each end of the profile; and the dip angle α. These parameters are calculated from a time distance plot such as the one shown in the upper part of the figure. The slopes on the plot, from which the apparent velocities are derived, are indicated along with the time intercepts of the high velocity arrivals, T_{iu} and T_{id}.

To construct a time-distance plot from which a model of the earth under the profile can be derived, all that is really needed is the times for the first arrival of seismic waves at each geophone. Under the conditions of a continuous profile, the first arrivals at the geophones close to the shotpoint are from the direct path, but to the more distant geophones the travel time is shorter by a refracted path than by a direct path. Accordingly, the first arrivals at these geophones are from the refracted paths. The arrivals are plotted in the manner of the upper part of Figure 9. There, the slopes of the lines through the plotted points are expressed in terms of apparent velocities.

Two shotpoints are required because the actual seismic velocity of a material cannot be obtained uniquely from refracted arrivals of waves that have traveled in

only one direction through it. The apparent velocity which is observed depends both on the actual velocity and the angle of dip of the interface from which the waves are refracted. Properly speaking, the dip angle is the apparent dip measured in incident plane; a subsurface refractor, for example, appears flat to a profile laid out parallel to the strike of the refractor. The apparent velocity is higher or lower than the actual velocity when the wave travels updip or downdip, respectively. The calculations for determining the actual velocity, the depth of the refractor, and the dip angle are derived and explained in Dobrin (1960, p. 81).

The conventional interpretation procedure must be modified because the field procedures used in this study are not the same as in the conventional method. The physical layout has been described in Figure 5 and the travel paths are shown in Figure 10. The geophones are not spaced over the length of the profile, but are relatively closely spaced in a group in the middle. They remain there until all shots for the particular profile have been recorded. Several charges are fired at various distances from each end of the geophone group. The shotpoint-geophone distances obtained in this way are the same as would exist in a conventional profile using only two shotpoints and a greatly increased number of geophones. A time-distance plot can be constructed using these

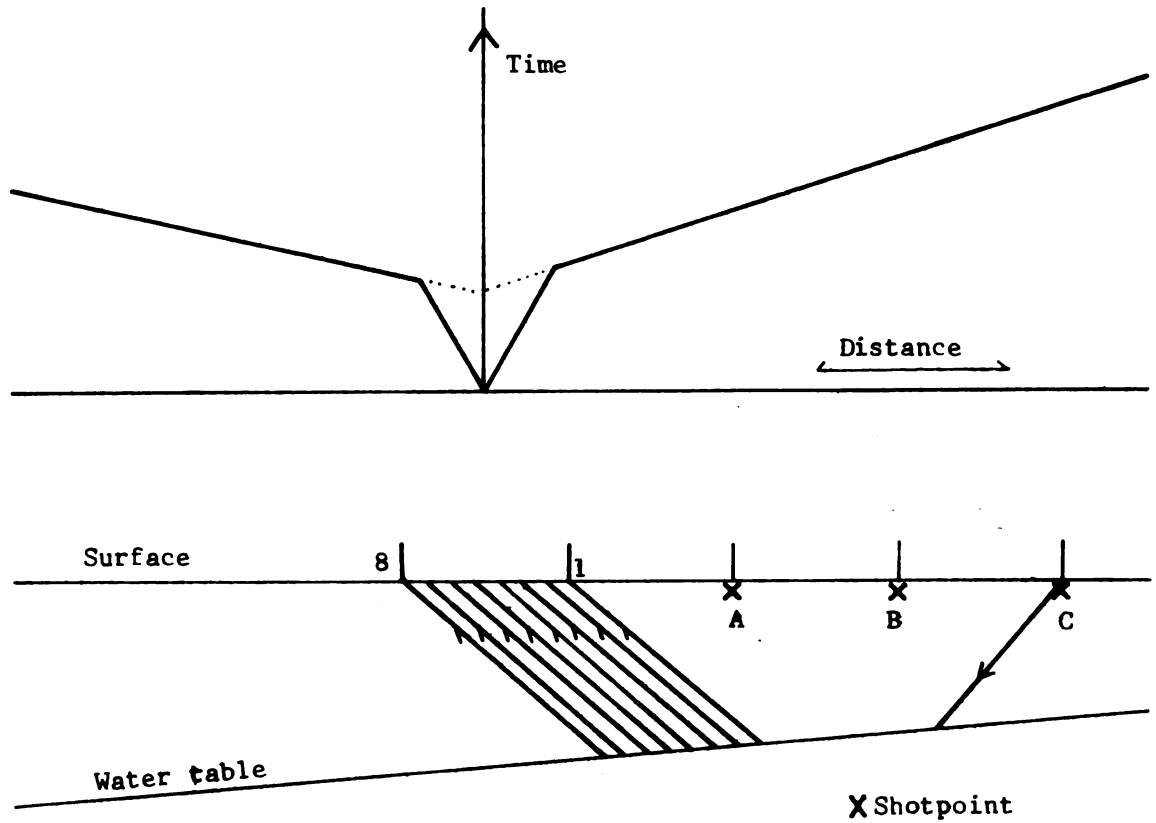

Figure 10.--Seismic refraction over a dipping layer in the modified method.

distances, but it cannot necessarily be interpreted in the usual way because the distances do not have the same meaning as in the conventional method. For example, in traveling 700 feet from shotpoint B to geophone 8, the wave does not take a path equivalent to the path from shotpoint C to geophone 1, also a 700-foot distance. The travel time for the former path must be greater because the path includes more low-velocity material. And neither path starts at the end of the profile, as it would in the conventional method.

A method of plotting a time-distance curve from data gathered in this manner is shown in Figure 10. The origin of the curve has been placed at the center, because the short geophone-shotpoint distances are physically near the center of the profile. Also, it would be inappropriate to have the curves cross over each other as they do in the conventional plot, because the waves traveling in opposite directions can have only a small part of their travel paths in common.

One way to treat the data is to consider the group of eight geophones as one geophone located in the middle of the geophone group. The arrival times at each geophone are picked as usual, and then a time is chosen to represent these picked arrivals at an imaginary geophone in the center of the geophone group. It can be seen in Figure 11 that the travel paths to the imaginary geophones resemble those of the conventional one-sided refraction profile

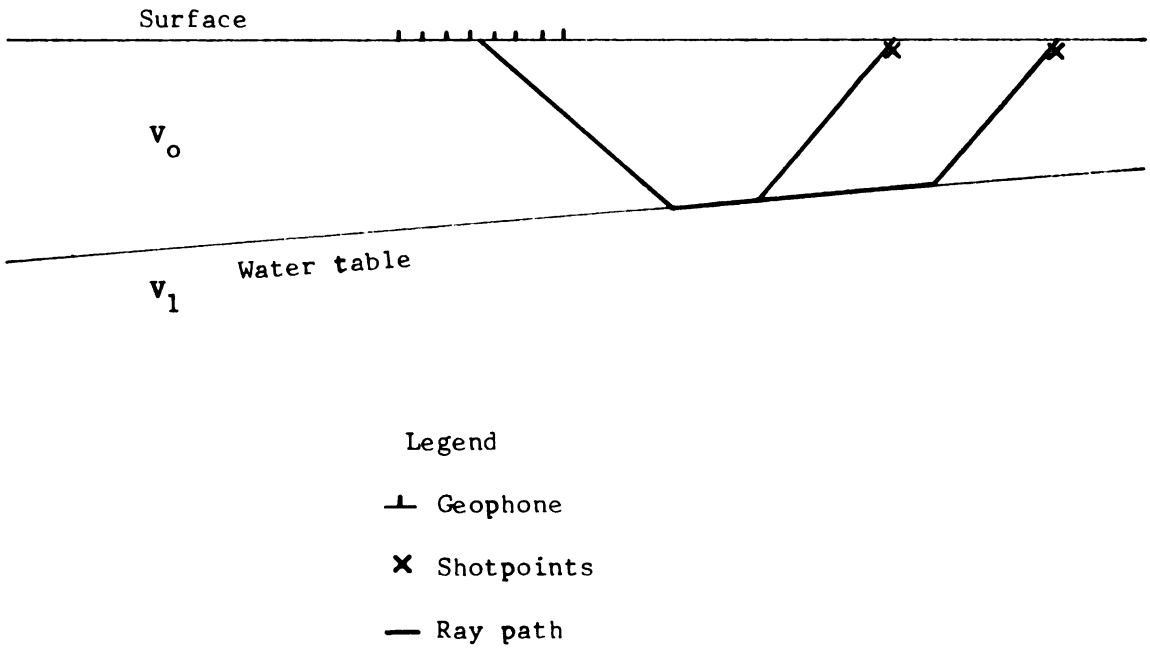

Figure 11.--Travel paths to the imaginary geophone of the "single-geophone" interpretation.

except that the geophone occupies the position of the single shotpoint, and vice versa, and that the direction of wave travel is reversed. The principle of reversibility states that the travel times would be exactly the same if the directions are reversed. Therefore a time-distance plot constructed on this basis could be interpreted in identically the same way as a plot from a conventional one-sided profile. It would have relatively few points plotted, but each point would represent data from eight geophones.

The above viewpoint suggests a method of checking the consistency of the data. The cross-spread velocities found from the shotpoints on one side of the geophones should be the same as the apparent velocities determined by using the "single-geophone" interpretation on the data from the shotpoints on the other side of the profile. The reversed direction of the wave travel imagined in the "single-geophone" interpretation is the same as the actual direction of travel on the other side of the profile. Therefore if the velocity and the dip of a refracting interface are unchanged under the profile, then both these velocities must be identical. Also, if the dip changes, then the two velocities must differ.

It is necessary to consider the possibility that the dip of the refracting interface is not consistent over the profile. For simplicity, we will consider that the interface has only one change in dip. There are then two cases.

First, the change in dip may appear on the time-distance curves as a discontinuity or a change in slope. In this case an anomaly would be recognized. But there is a possibility of a change in dip not causing an anomaly on the curves. This can happen if the change in dip is physically located close enough to the center of the geophone group so that arrivals to only a few, or perhaps none, of the geophones are affected by it. The slanting upward paths (at the critical angle) of the refracted arrivals leave an area directly underneath the geophone group (see Figure 10) which does not contribute to the refracted arrivals. This area can be quite large if the refracting interface is deep.

It should be noted that since the depth to the refractor at the center of the geophone group is common to both the updip and downdip shots, the intercept times are identical for both shots. This is rigorously true as long as the dip is constant under the profile.

The possibility of an unrecognized change in dip leads to some ambiguities in the interpretation of the refracted arrivals. The two apparent velocities, derived from waves traveling in opposite directions, are treated as coming from a single refractor with a constant dip. If in fact they come from two segments of the refractor, each with a different dip, then the calculations based on a constant dip must be in error. For example, in the case of a refractor which appears convex upwards, the two

apparent velocities are lower than they should be. As a result, the calculated velocity is lower than the actual velocity, and the calculated depth is less than the actual depth. The reverse is true when the refractor appears concave upwards. But in both cases the dip calculated for a single refractor is approximately correct as an average dip over the length of the profile.

In the Udell field area, the only interface deep enough to have an unrecognized change in dip in this manner is the bedrock surface. But since this interface is not very significant to the conclusions of this study, the possibility of serious error resulting from an unnoticed change in dip is believed to be remote.

Picking of Arrival Times

To plot the time-distance curves from which a simple refraction model can be constructed, all that is really necessary is to "pick" first arrivals from the seismograms. However, it is very often possible to improve the accuracy of the lines drawn through the plotted first arrivals by recognizing some arrivals that come in after the first one. However, it is usually easier to pick first arrivals than later ones, because the first arrivals are not confused by other signals.

"Picking" a seismic record is something of an art. It is usually desired to identify the time of the very first disturbance caused by the oncoming wave. However,

it is often very weak, and what is picked is frequently a slightly later and stronger cycle. Usually, this is not of great consequence. Similarity between adjacent traces is the most important criteria for recognizing an arrival. The other principle criteria are a change in the character of the signal and a sudden increase in its energy. Methods of picking seismic records are discussed at some length by Jakosky (1950, pp. 699-709).

Interpretation from Refraction Arrivals

The time-distance plots for Sites One, Two, and Three are shown in Figures 12, 13, and 14. These plots were constructed using arrival times picked from the vertical geophone traces on the original seismograms. The velocities shown for the surface layer range from 850 to 1050 feet per second. It will be shown later that the velocity appears to be about 1150 ft/sec and that the picked lower velocities may represent a surface wave with lower velocity but greater amplitudes than the direct wave. Arrivals for a second layer with a velocity between 5000 and 6000 ft/sec are also shown. This layer is identified as the saturated zone. A third layer appears on the plots for Sites Two and Three with apparent velocities between 12000 and 13,500 ft/sec. This layer is identified with the bedrock.

An actual velocity of 5700 to 5900 ft/sec is consistent with the apparent velocities measured at the field sites, with one exception. The actual velocity of a dipping

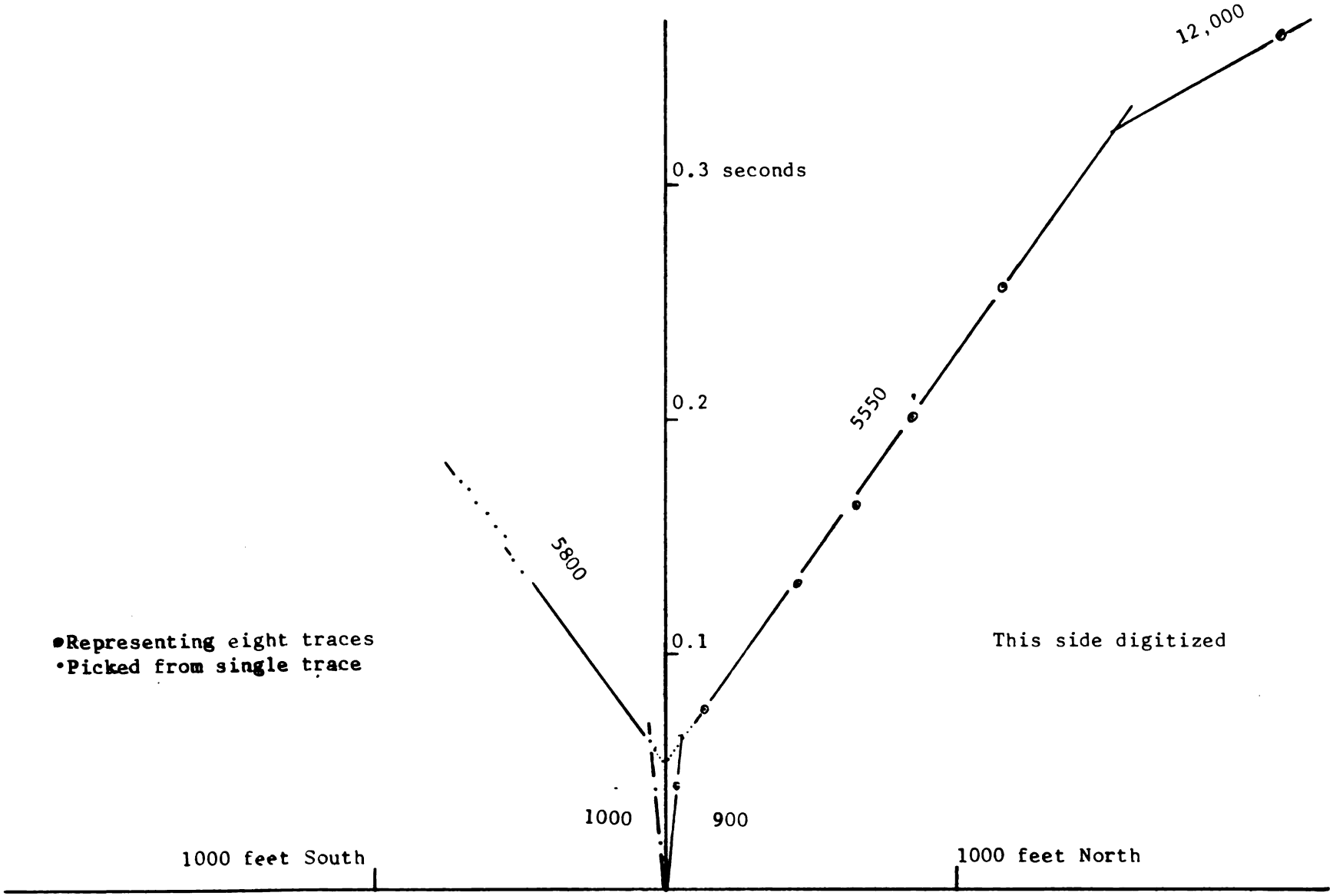

Figure 12.--Time-distance plot for Site One.

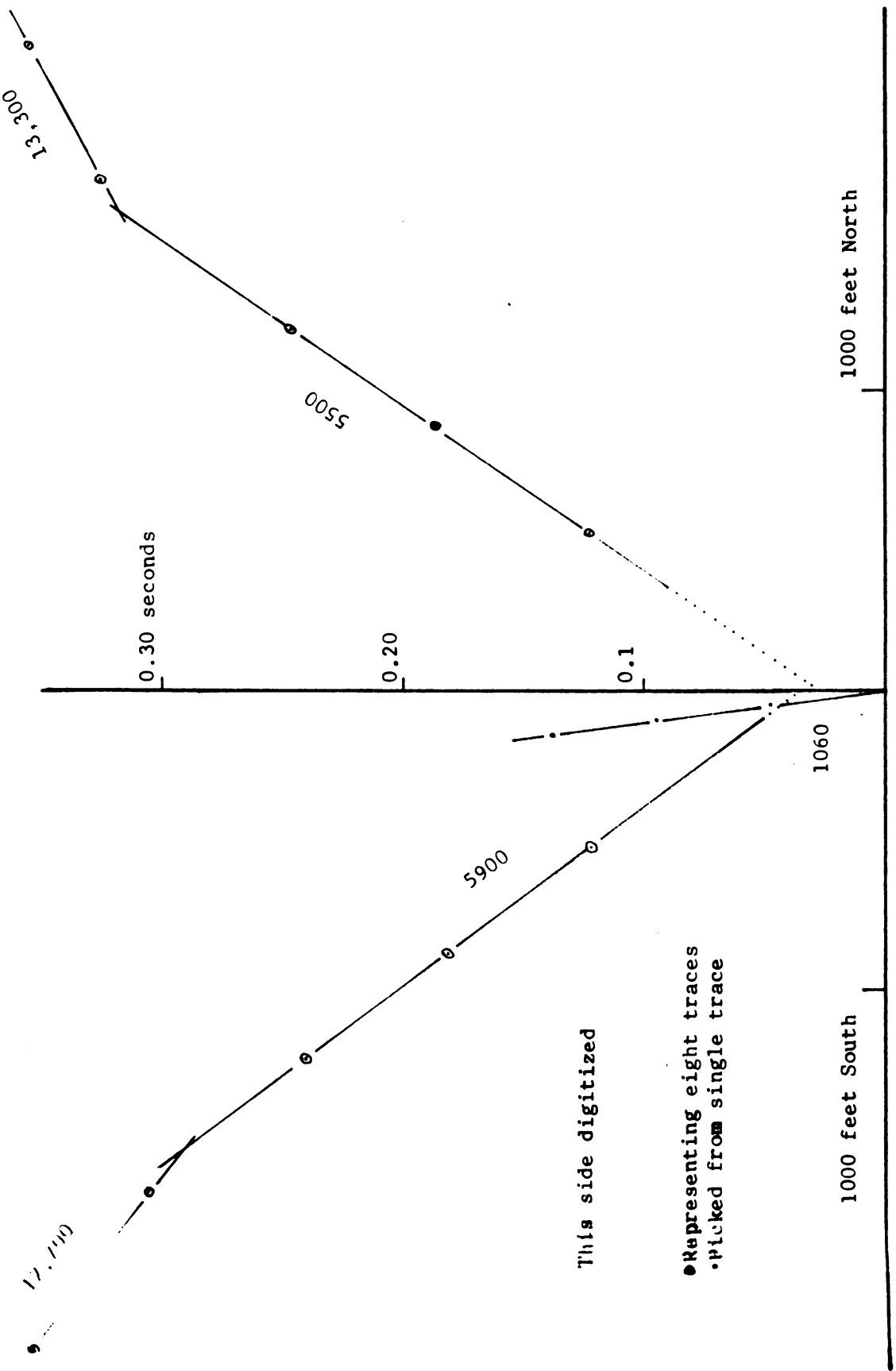

Figure 13.--Time-distance plot for Site Two.

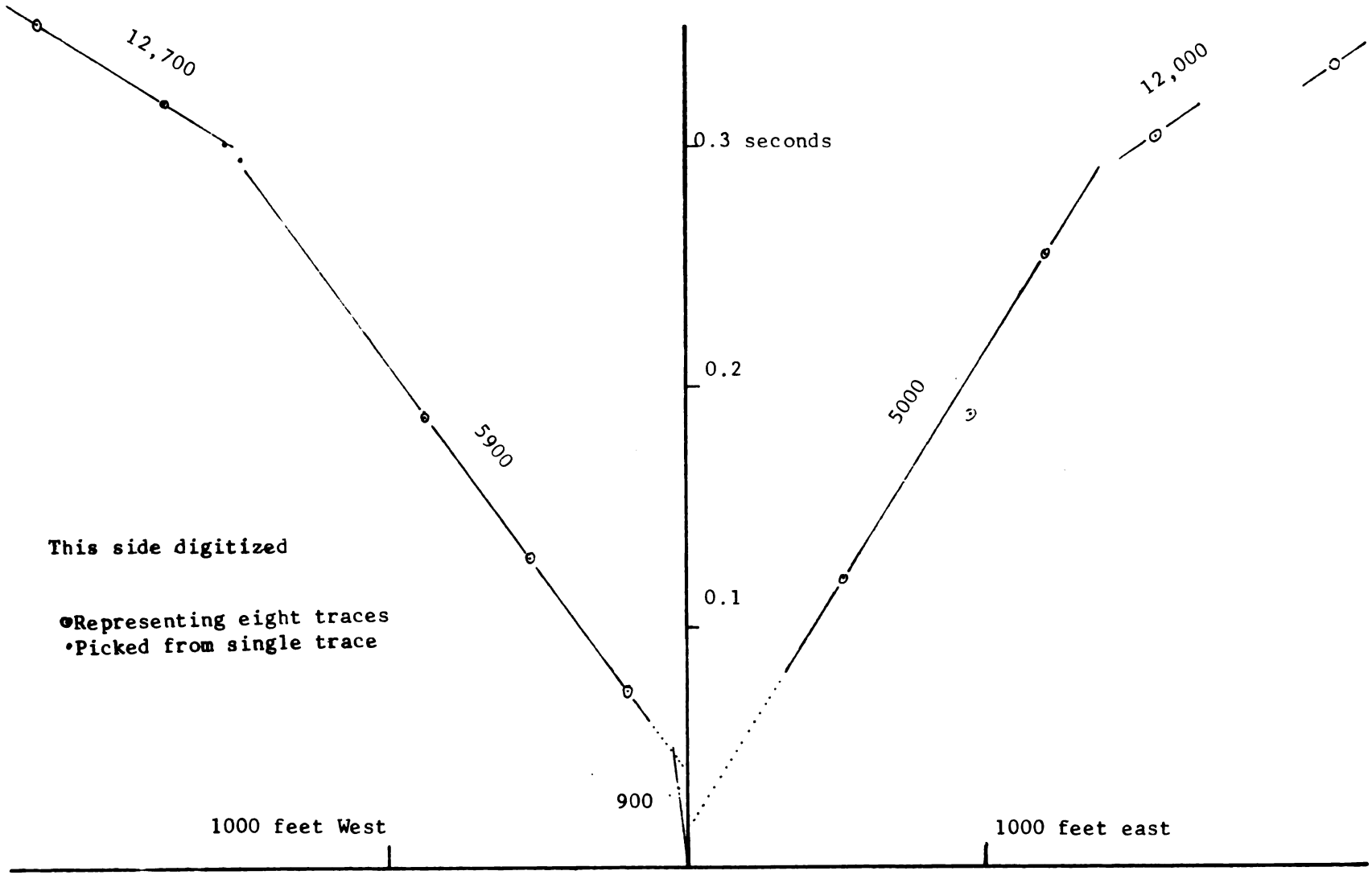

Figure 14.--Time-distance plot for Site Three.

layer can be closely approximated by the average of the apparent velocities in opposite directions, provided that the dip and composition of the layer are unchanged under the profile. The apparent velocities in three directions at Sites Two and Three are nearly equal, but 5000 ft/sec was measured at the east end of Site Three. Because the velocity on the opposite side of the site agrees with the velocity measured at the adjacent Site Two, it seems that the lower velocity is anomalous. Another indication that this velocity is anomalous is the fact that the intercept times do not agree at Site Three. However, it must be assumed that the anomaly is the result of a lateral change in the sediment, because the amount of dip needed to create the observed difference in velocity greatly exceeds the maximum possible dip of the water table allowed by the water table measurements at test wells.

Similarly, the apparent velocity for the bedrock of 13,300 ft/sec at the north side of Site Two is probably anomalous. The actual velocity is probably close to 12,500 ft/sec, as reported in a more recent study by Bennett (1970). The differences could be due to a lateral variation in the bedrock or more likely to dipping interfaces caused by bedrock topography.

The depths for the water table were calculated from the seismic data and compared to the depths from test wells. For Site One, the calculated depth of 30 feet agrees closely with a measured depth of 32 feet from a

test well. Sites Two and Three were considered together for calculation of the depth to water table because of their close proximity and similarity of seismic data. Their depth is calculated to be 17 feet. This agrees moderately well with the 20 feet and 14 feet measured at test wells at Sites Two and Three, respectively. The well data indicates that the depth is somewhat variable, and in fact at the south end of Site Two it is only 5 feet. However, neither of the test wells for these sites is located near the geophone groups.

The refraction profiles as used in this study have been used to measure the velocities of the materials of the three layers and the depths to the interfaces between these layers. The geology of the field area appears to meet the conditions required for interpretation of the data by conventional refraction calculations, although some exceptions have been noted. The materials encountered and their compressional velocities are as follows: unsaturated sand, about 1150 ft/sec; water-saturated sand, about 5700 ft/sec; and the Mississippian sedimentary rocks, about 12,500 ft/sec. The water table is 30 feet deep at one site and about 17 feet deep at the other two sites.

CHAPTER VII

ANALYSIS OF THE SEISMIC DATA

Introduction

In the Udell field area most of the seismic energy resulting from an explosion in a shothole is confined to the relatively thin unsaturated layer. The energy travels by multiple reflections within the layer, which is bounded by the earth's surface and the water table, in a manner similar to the transmission of microwave radiation through a waveguide. Therefore, associated with the direct arrival are arrivals from multiply reflected paths in the unsaturated layer. Because these arrivals have traveled over paths of different lengths, all longer than the direct path, they follow the direct arrival by different time intervals. These arrivals constitute a surface wave which does not appear to have been reported in geophysical literature, although it resembles some well-known surface waves.

The direct arrival is more clearly seen on the plots of absolute signal magnitude than on the original seismograms. The direct arrival at 1150 ft/sec is very weak and hard to recognise on the original seismograms. What has been picked as the direct arrival on these records

is a later arrival, coming at times corresponding to about 1000 ft/sec. However, the direct arrival can be recognised on the absolute magnitude plots as the beginning of a long wavetrain, even from signals recorded at considerable distance from the shotpoint.

The Unsaturated Layer as a Wave Guide

Seismic energy leaves a shotpoint as an expanding sphere of compressional waves, whose spherical shape is distorted upon reaching the surface or an interface with another material. All of the seismic energy which reaches the surface is reflected, because none can be effectively transmitted into the air. The energy reaching the water table may be divided, part being refracted through the water table into the saturated zone and part reflected back into the unsaturated layer. How the energy is divided depends on the incident angle of the rays as they strike the water table and the density, compressional velocity, and shear velocity of each material.

A compressional wave striking the water table at an incident angle greater than 15 degrees cannot be transmitted as a compressional wave into the saturated zone. This is the critical angle, ϕ_e, calculated from compressional velocities of 1150 ft/sec and 5700 ft/sec, above and below the water table, respectively. However, some energy may be transmitted as shear waves into the lower medium by conversion at the water table. Probably no critical angle

exists for this conversion, since the best estimate of the shear velocity in the saturated zone is less than the compressional velocity of the saturated sand. Therefore, if this is true, compressional waves incident at any angle may generate shear waves which are transmitted into the saturated sand. Figure 15 shows shear waves entering the saturated zone by this means. Shear waves are also shown being transmitted through the water table with little change in direction. This would be the case for a small shear velocity contrast across the water table.

The shear velocity in the saturated sand has not been firmly established. For the present purposes, it will be assumed that the shear velocity in the saturated sand is about the same as it is in unsaturated sand, i.e., about 600 ft/sec. This seems reasonable in view of the study by Harris and Gardner (1968, p. 12) who report a 5 per cent decrease in shear velocity in saturated sand as compared to dry sand. But on the other hand, there are some indications from a later study in the same area that the shear velocity may be in fact higher in the saturated zone and on the order of or slightly faster than the compressional velocity in the unsaturated sand. However, this shear velocity does not affect the treatment of the multiply reflected waves in the unsaturated zone.

Shear waves are generated in the unsaturated layer whenever compressional waves (with some incident angles

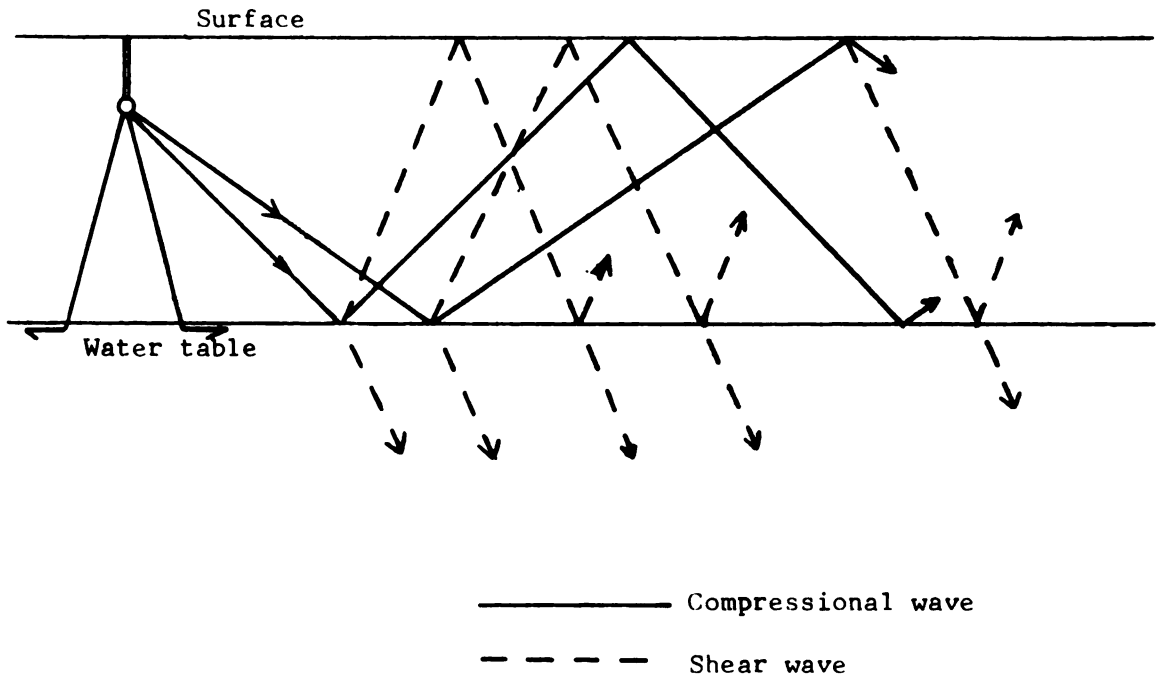

Figure 15.--Shear waves entering the saturated zone.

possibly excepted) are reflected from the surface or from the water table. The incident compressional wave, the reflected compressional wave, and a reflected (by conversion) shear wave are all in the unsaturated layer, so their angles are governed by their velocities in this material, in accordance with Snell's Law. However, the amplitudes of the waves generated as a result of the incident compressional wave do depend on the velocities below the water table. The amplitude ratios have not been calculated because they are dependent, among other things, on the shear velocities, which are not well-known, and also on the incident angle in a manner that would be hard to explicitly describe.

The shear waves, generated by conversion of a reflection, are present throughout the wave guide shortly after the passage of the direct wave and continue to be generated for some time afterwards. Provided that the distance from the source is reasonably large, many paths for multiply reflected arrivals exist, each with a different number of reflections and therefore with different locations for the reflection points. Shear waves may be generated from each of these reflection points. Because some of the multiply reflected wave paths are considerably longer than the direct path and have correspondingly greater travel times, compressional pulses from the explosion continue to arrive for some time after the passage of the direct arrival.

Therefore shear waves continue to be generated by the reflections of the compressional pulses from the boundaries of the wave guide. The particle displacements, a composite of shear and compressional movements, must then be complex in form.

Travel paths for compressional arrivals and shear arrivals due to conversions are shown in Figure 16 for cases involving one reflection (PP and PS) and three reflections (PPPP and PPPS). Other wave paths, not shown, are those which have four or more reflections, those whose first reflection is from the surface rather than the water table, and those involving one or more reflections of the generated shear wave.

Two important consequences arise from the application of Snell's Law to a shear wave generated by a compressional wave conversion. The emergent shear wave rises at a small angle of reflection, because of the large velocity contrast between the compressional and shear waves. The angle of reflection is almost constant; compressional waves with incident angles between 60 and 90 degrees generate shear waves with angles of reflection between 25 and 28 degrees. Second, the shear waves travel only a short distance to reach the surface, so that their arrival is not greatly delayed by their slower velocity.

Only the energy contained in a 15 degree vertical cone can be injected into the saturated zone by refraction

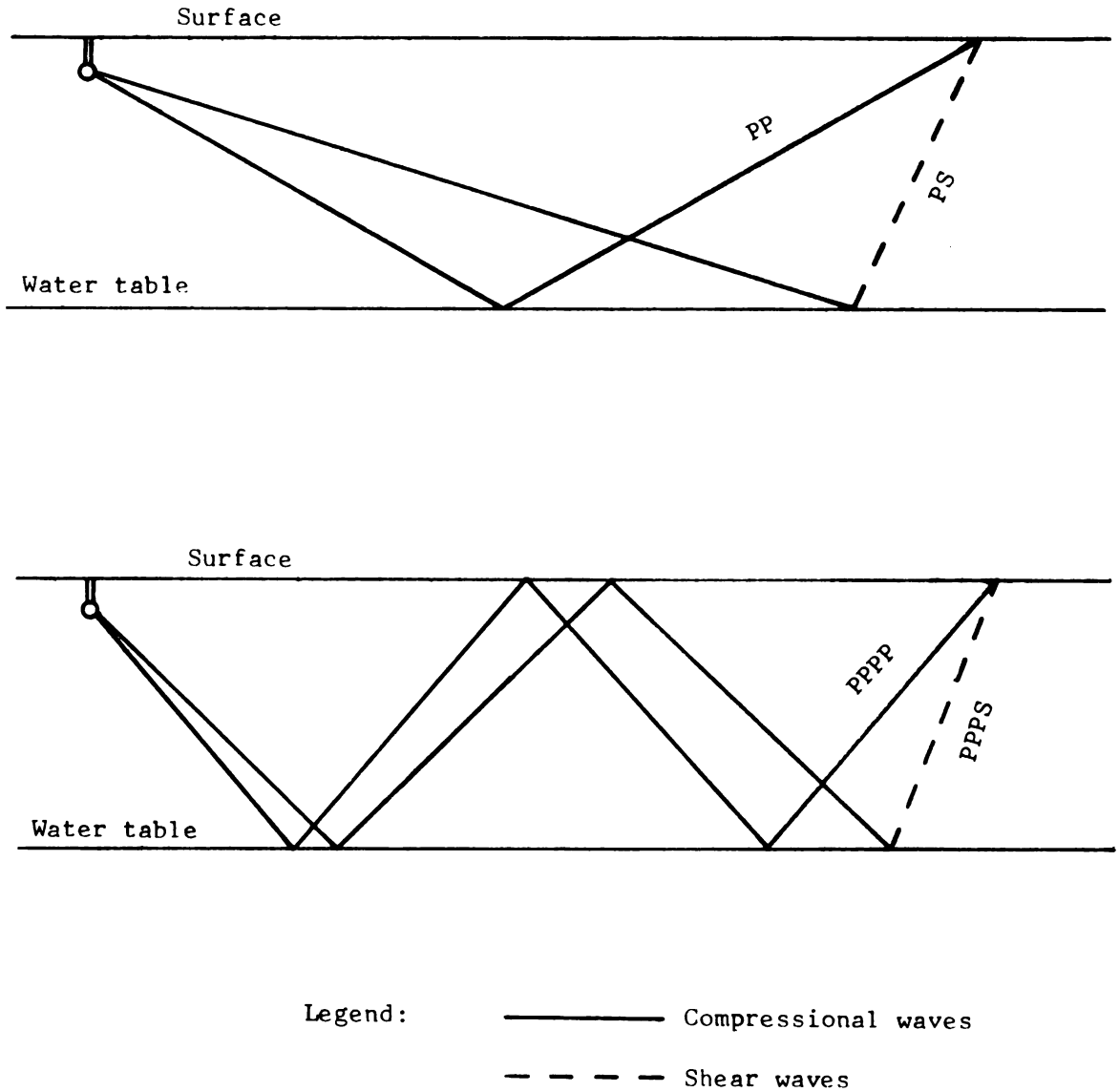

Figure 16.--Shear and compressional waves reaching the same point by slightly different paths.

of compressional waves through the water table. Therefore it is expected that 92 per cent of the compressional energy generated by the explosion is initially channeled into the unsaturated layer. Compressional waves with greater angles of incidence are totally reflected, with a small portion of energy probably being lost due to generation of shear waves in the saturated zone. As indicated earlier in connection with Figure 15, downward traveling shear waves in the unsaturated layer, either generated at the surface by conversion from compressional waves or generated at the water table and reflected from the surface, are probably transmitted into the saturated layer with little change in direction because of the assumed small contrast in shear velocities across the water table. However, the density contrast is considerable, and it must cause some reflection back into the unsaturated zone.

It can be expected, then, that considerable energy may be propagated through the surface layer by multiple reflections from the boundaries of the layer. The mode of propagation thus resembles the Love wave or the normal mode propagation in shallow oceans described, for example, by Officer (1958, p. 117ff).

The Direct Arrival

The following charts each contain the absolute signal magnitude plots for one site. In each case, the plots show data from shotpoints on only one side of the geophone group.

The traces are plotted so that the distance of each line from the top of the chart is proportional to the corresponding shotpoint-geophone distances. In this way, correlation lines drawn through picked arrivals are scaled as segments on a time-distance plot. The chart for Site One is Figure 17; for Site Two, Figure 18; and for Site Three, Figure 19.

The refracted arrivals are not prominent on the absolute signal magnitude plots. These arrivals have the high cross-spread velocity of the saturated zone and correspondingly small travel times. However, they can be easily recognised on the original seismograms. It is thought that this is because the digitisation process does not record low amplitude, high frequency signals with the same fidelity as the higher amplitudes and lower frequency signals of the later arrivals. Because the sampling is no better than once every three milliseconds, fewer points are recorded in each frequency of a higher frequency signal than a low frequency signal. Also, the human error in positioning the reading pencil is greater in proportion to the shorter periods of the higher frequency signals.

Four lines have been drawn across each of the plots, each line representing a picked seismic arrival. The apparent velocity of each arrival is shown; in order of decreasing velocity, the arrivals are the refracted wave from the saturated layer, the direct wave, the surface wave related to the direct wave, and the Rayleigh wave.

Certain arrivals are more conspicuous in some record groups than in others at Site One because of the unequal gains used in recording the different shots. The direct arrival was picked primarily from the records at distances from 1210 to 1360 feet where the high amplitudes made it prominent. It is also seen on several traces from the most distant shot (2060-2210 feet), but is too weak to be seen on the low amplitude records for 810 to 1160 feet. The surface wave can be seen in these low amplitude records, and it can also be correlated with an increase in energy in several traces from the most distant shot. The Rayleigh wave is seen as the beginning of a wave train on the traces for distances from 810 to 1160 feet. The digitisation of the group of traces from 1010 to 1160 feet was stopped at the point where it became difficult to follow the traces through high-amplitude swings. This apparently marked the arrival of the Rayleigh wave. The refraction arrival is indicated at 5500 feet/sec as picked from the original records. The apparent velocities of the other arrivals are as follows: direct wave, 1120 feet/sec; surface wave related to the direct arrival, 980 feet/sec; and Rayleigh wave, 560 feet/sec.

The arrivals at Site Two are more consistent in amplitude. The direct arrival was picked at 1180 feet/sec on the basis of an increase in amplitude. The surface wave at 1020 feet/sec is apparent as the beginnings of wave

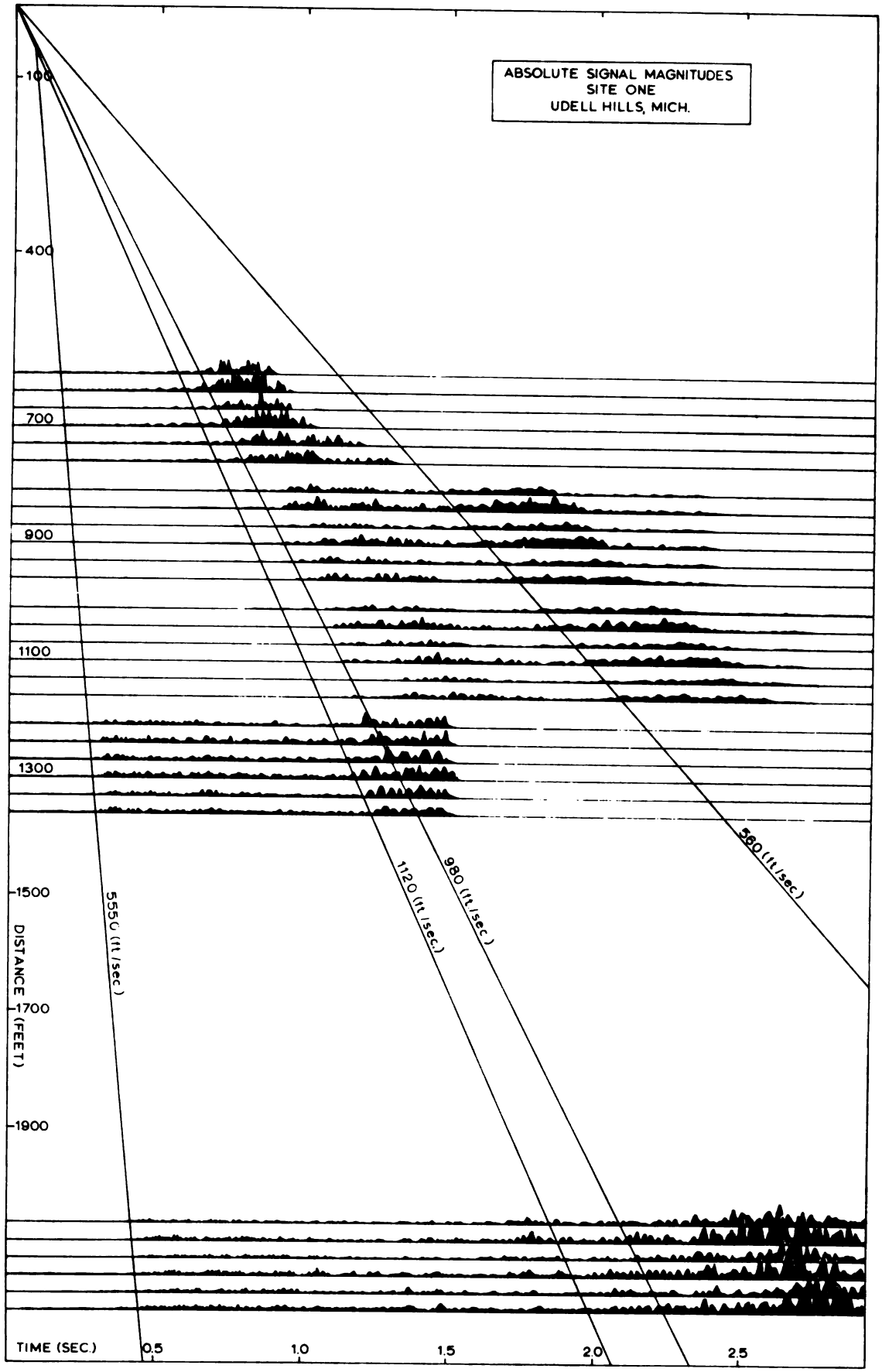

Figure 17.--Site one plot.

trains at short distances and a change in character at greater distances. The Rayleigh wave, picked at 550 feet/sec, shows small character changes at distances from 700 to 900 feet and the beginnings of a wave train at distances from 1150 to 1400 feet. The refracted arrival, with an apparent velocity of 5900 feet/sec, was picked from the original records.

As might be expected from the close proximity of the two sites, the velocities at Site Three are similar to those from Site Two. The direct arrival was picked at 1170 feet/sec, primarily from increases in energy. The surface wave was picked on the basis of a change in character to an "elliptical" motion at short distances but at greater distances is more apparent as an increase in amplitude. Its velocity is 1040 feet/sec. The Rayleigh wave, at 550 feet/sec, was picked with difficulty from changes in character and amplitude. The refracted arrival again came at 5900 feet/sec velocity.

The absolute signal magnitude plots show a higher velocity for the direct arrival than the velocity picked from the original vertical component records. Velocities of about 1150 feet/sec and 1000 feet/sec were obtained from the computed plots and the original records, respectively. The lower velocity can be seen on the absolute signal magnitude plots to be that of a later and stronger phase associated with the direct arrival, i.e., the guided wave. The

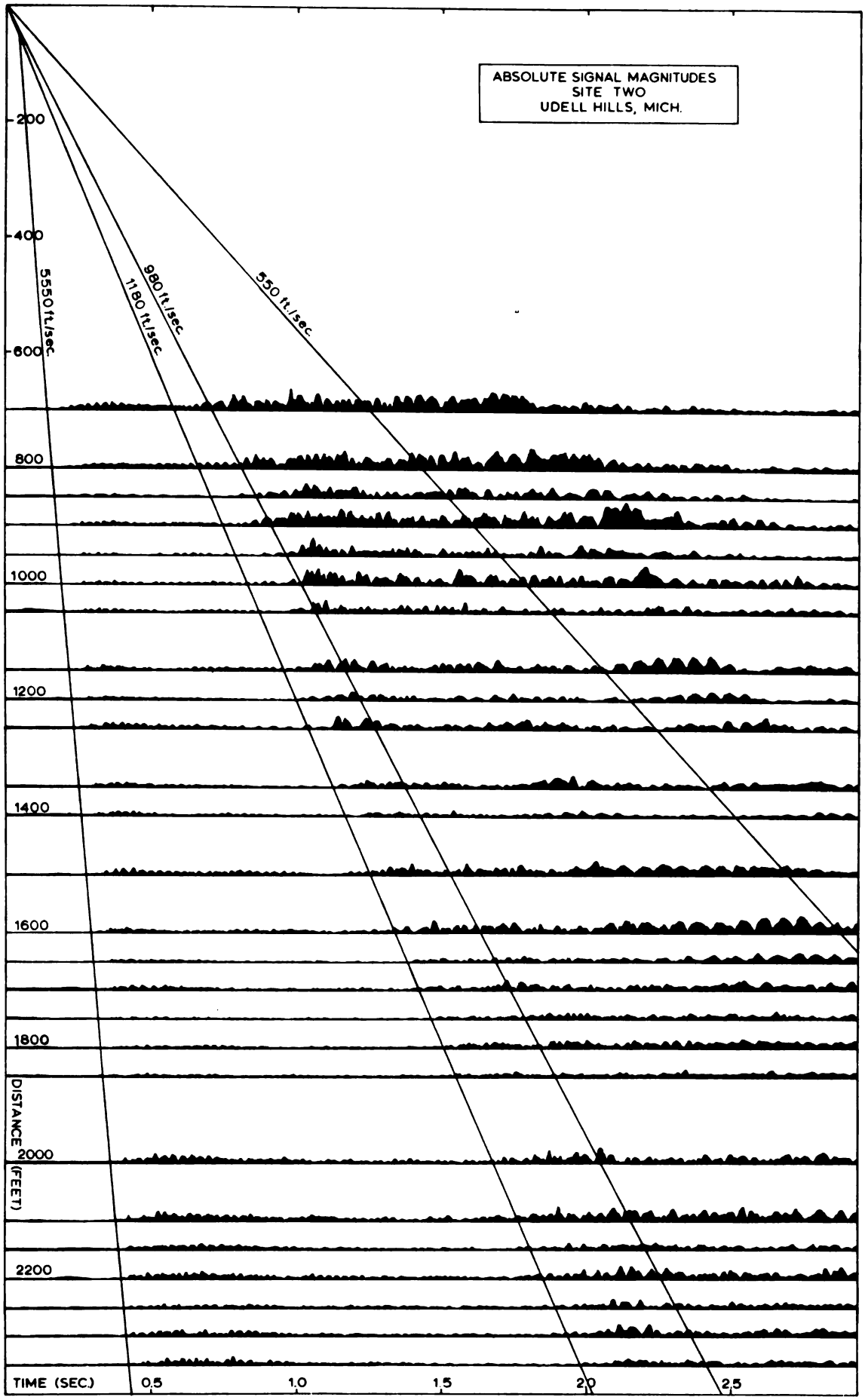

Figure 18.--Site two plot.

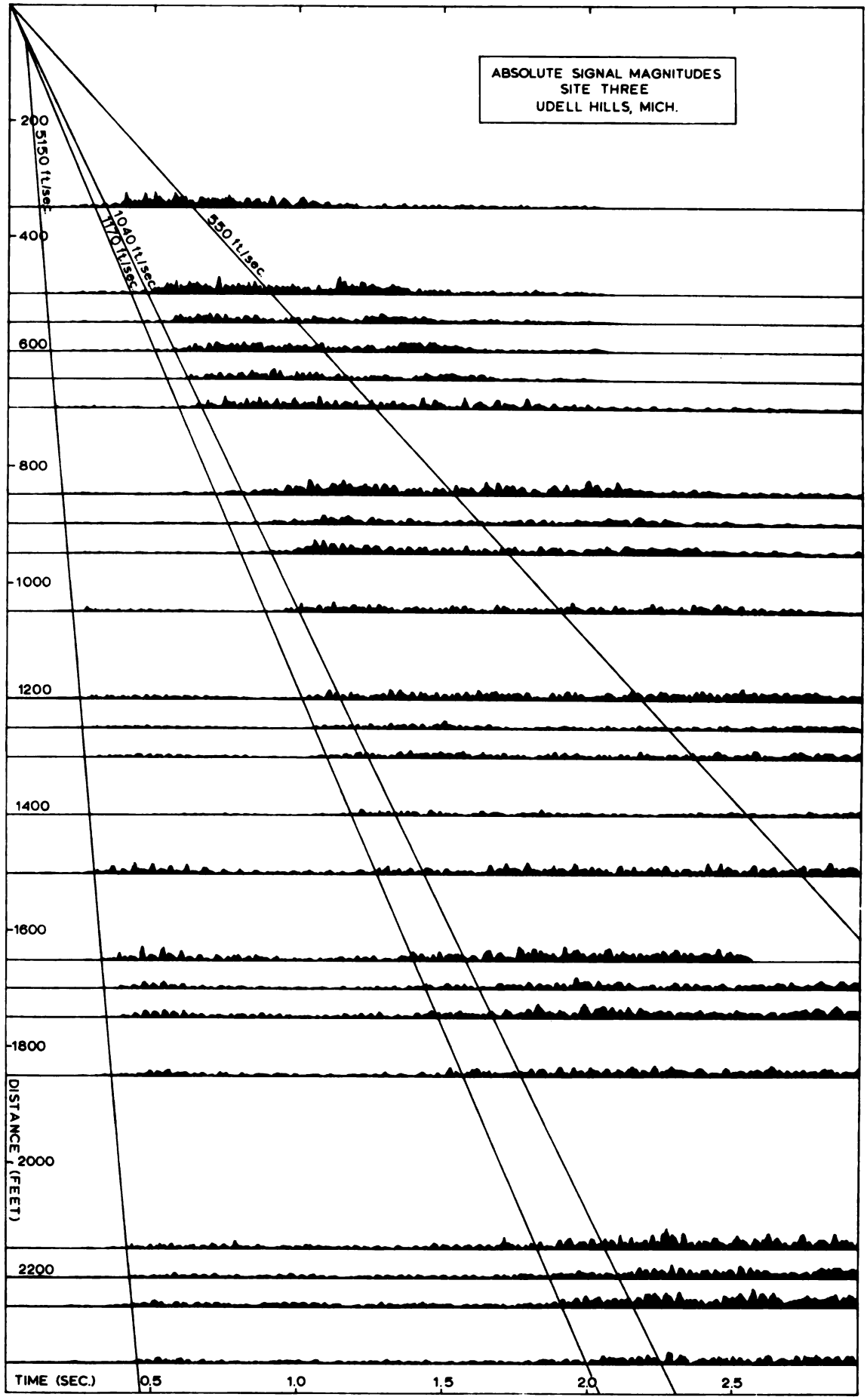

Figure 19.--Site Three Plot.

higher velocity is confirmed from a few of the original records at Site One, where the direct arrival can be picked at the higher velocity for short shotpoint-geophone distances.

Figure 20 is a comparison of the absolute value plots with the original seismic data for a Site Two shot. The geophone spacing is 50 feet and the closest geophone is 1500 feet from the shotpoint. Starting at the top of the figure, the four groups of eight traces each are the computed absolute signal magnitude plots, and the HL, vertical, and HT components of motion. The original data presented here is in the form of plots drawn from the digitised data. One trace, the vertical component of the second geophone, was not digitised because it was dead on the original record. The picked arrival times for the direct arrival are shown as lines across each group of traces.

Success in picking the direct arrival from the absolute signal magnitude plots shows that these plots are an improvement over the original data for the recognition of the direct arrival. It can be seen, however, that the direct arrival could have been picked from the HL components. This is an after-the-fact observation, because the direct arrival was not recognised on the original seismograms until its arrival time was known.

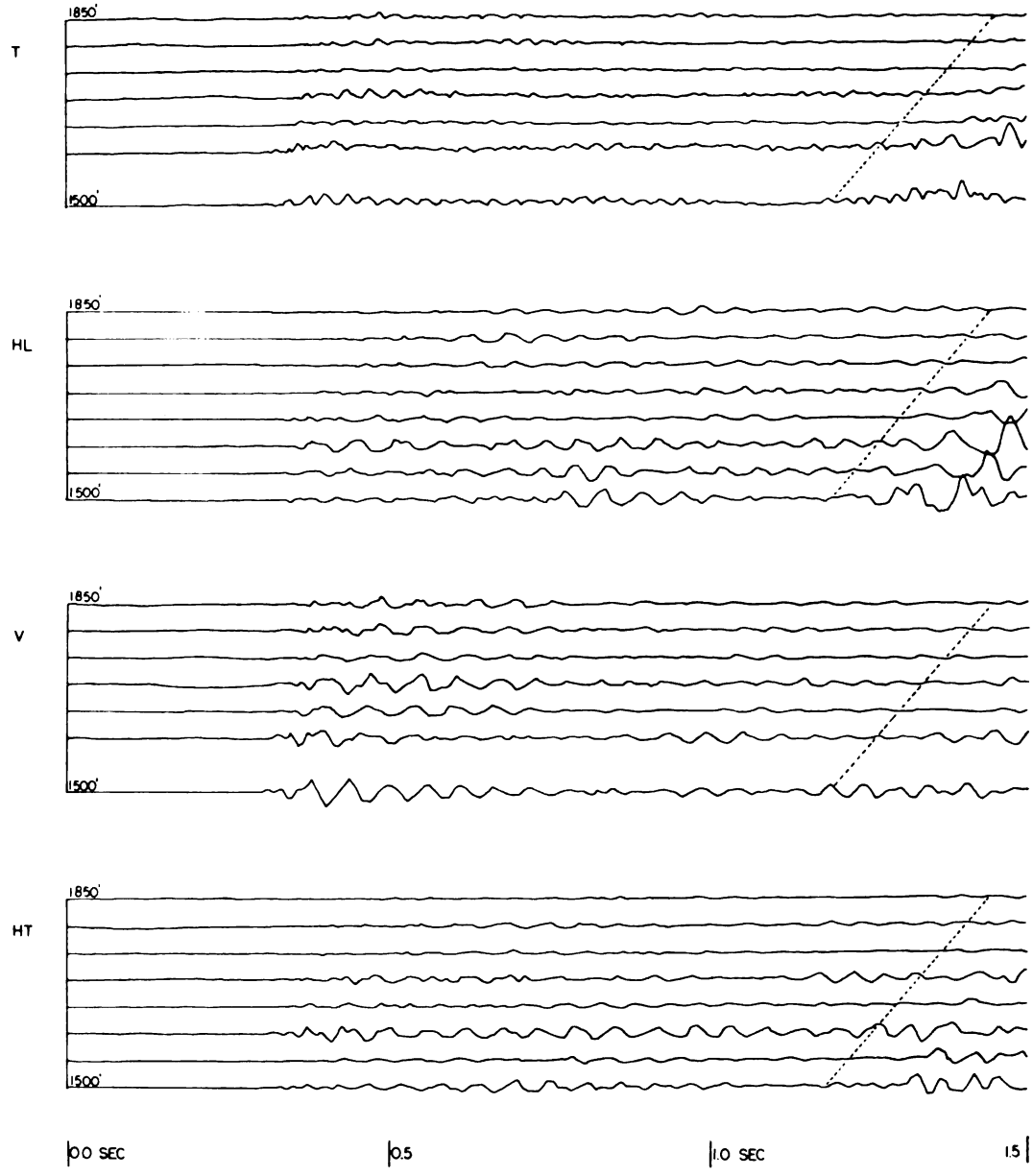

Figure 20.--Comparison of the computed absolute signal magnitude plots with the original data.

The Surface Wave Related to the Direct Arrival

A change in the character of the signals of many of the absolute signal magnitude plots can be seen at a time about 15 per cent later than the direct arrival time. The change is from "rectilinear" motion to "elliptical" motion, as these terms are defined earlier. This change marks the beginning of the surface guided wave related to the direct arrival.

A wave traveling by multiple reflection through a horizontal wave guide must have a longer travel path than the direct arrival, because the multiply reflected wave travels at an angle to the horizontal. It is easy to calculate that a travel path elongated by 15 per cent is one whose segments have angles of incidence of about 60 degrees. Compressional waves have particle motion parallel to the direction of propagation, so that the particle motion of a compressional wave taking such a path is also 60 degrees from the vertical.

Figure 21 illustrates the relationship between the particle motion of these compressional waves with that of the shear waves. The shear waves have been seen earlier to have an angle of reflection of very nearly 30 degrees from the vertical, and their particle motion is perpendicular to that direction. The two waves arise from compressional waves that have traveled very similar paths. Therefore, their waveforms should closely resemble each other, so that

interference is possible. As shown in the figure, the two directions of motion are about 60 degrees apart. The resultant of the two motions must be elliptical particle motion except in the fortuitous case of the two motions being exactly in phase. In general, this is not the case because the two transit times--along slightly different paths with different velocities in the final segments--are unlikely to be identical.

The interaction of the compressional and shear motion is proposed as the mechanism for the "elliptical" motion observed on the absolute magnitude plots. It is impossible at the present time to do a rigorous analysis of the resultant particle motion predicted on a theoretical basis from the characteristics of the wave guide because much of the necessary information is not quantitatively known. This includes the relative amplitudes of all compressional and shear waves and their phase relations, which depend on the reflection proporties and path lengths within the wave guide. The reflection properties and relative amplitudes could be determined from the Zoeppritz equations (Richter, 1958, p. 670) if densities, compressional velocities, and shear velocities were known for both materials. The necessary data is not available. Also, a rigorous analysis would require the consideration of many more wave paths than those shown in Figure 21. Without a rigorous analysis, the wave type is identified on the basis of its observed

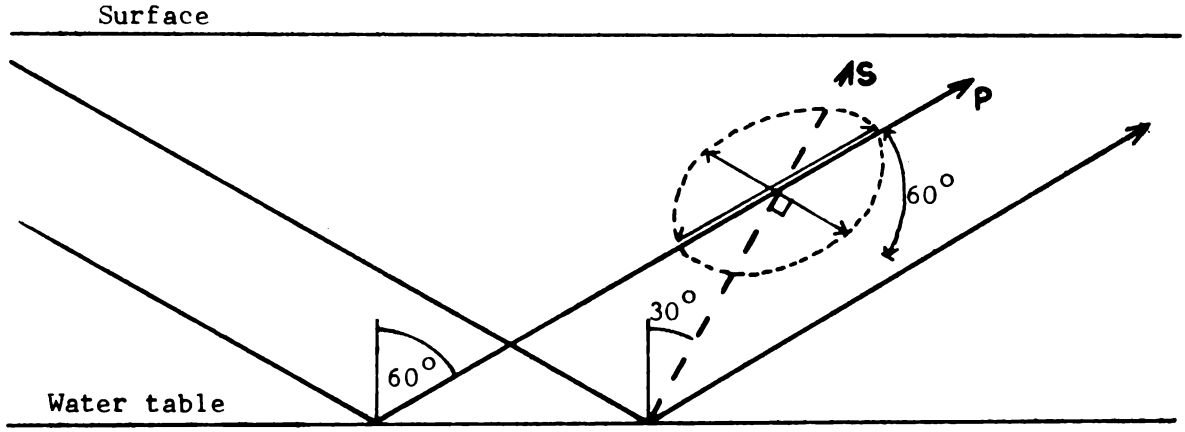

Legend ——— Compressional waves

— — — — Shear waves

a possible path of particle motion, the sum of the motions of the compressional and shear particle motions

Figure 21.--The "elliptical" wave motion as the sum of compressional and shear motion.

energy, velocity, and particle motion, which are in qualitative agreement with seismic theory.

The analogy between the proposed surface wave and the Love wave or oceanic normal mode propagation is not perfect, principally because in each of the latter two wave types, only one kind of wave is involved in the multiple reflection paths. The Love wave is composed exclusively of horizontally polarized shear waves, and the oceanic normal mode propagation is composed exclusively of compressional waves. In the proposed propagation mechanism, both compressional and shear waves are available and can account for the observed motion.

The observed surface wave does not appear to have been reported in the literature. It probably cannot exist except when the conditions favor the channeling of so much energy into a surface layer. Following the direct arrival as it does, it is in a portion of a received wave train that is commonly overlooked as noise in seismic investigations. This surface wave, like other surface waves, must carry information about the surface layer. An investigation into the characteristics of the observed wave might lead to a new way of determining the thickness of the layer, some physical properties of the surface material, and possibly some information about the underlying material.

The Multiply Reflected Refraction Arrival

Some theoretical predictions about the nature of seismic reflections at normal or near normal incidence are confirmed by experimental evidence from seismic records. Compressional waves undergo a phase change of π in reflection from a free surface (i.e., the earth's surface) and no phase change on reflection from an interface with a material having a higher compressional acoustic impedance. The saturated sand has a much higher acoustic impedance than the unsaturated sand, because both density and velocity are higher in the saturated sand.

The refraction arrival from the saturated sand provides a seismic wave at near-normal incidence to test the theory. The ray traveling horizontally in the saturated sand is refracted through the interface at the critical angle, 15 degrees from the vertical. Traveling upward through the unsaturated zone, it strikes the surface and is totally reflected. Then it travels downward, again 15 degrees from the vertical, and is reflected so that it again travels upward. Thus several reflections between the surface and the water table may occur to the same wave arrival. The energy loss in the reflections at the water table may be expected to be small because the wave reflects at the critical angle.

The refracted wave arrival resembles a pulse. Therefore the arrival time and phase can be easily recognised.

These characteristics make it easy to study the phase relations of the refracted arrival as it is reflected between the boundaries of the unsaturated layer.

Figure 22 shows diagramatically the travel of a pulse as described above. We will consider a pulse refracted upward at point A and label its phase artibrarily positive with a plus sign. At point B it is reflected downwards, so its phase is labeled minus. When this pulse is reflected from the water table at point C, it undergoes no phase change, and its phase is still labeled minus. At point D, it is reflected down again, and this time with a phase change because of the free surface. Its phase is again labeled plus. After being reflected again from the water table with no phase change at point E, it reaches point F as a pulse with its phase still labeled plus. The argument is unchanged whether the first pulse is actually a compression or a rarefaction.

The pulses received at any point on the surface alternate in phase. In the figure, three pulses are received at point F. The first one to be received has traveled through the saturated zone and has been refracted upward at point E. The second pulse received is refracted upward at point C and then reflected twice with one phase reversal along the path CDEF. The third one is refracted upward at point A, travels path ABCDEF with two phase reversals, and therefore reaches point F with the same phase it had originally.

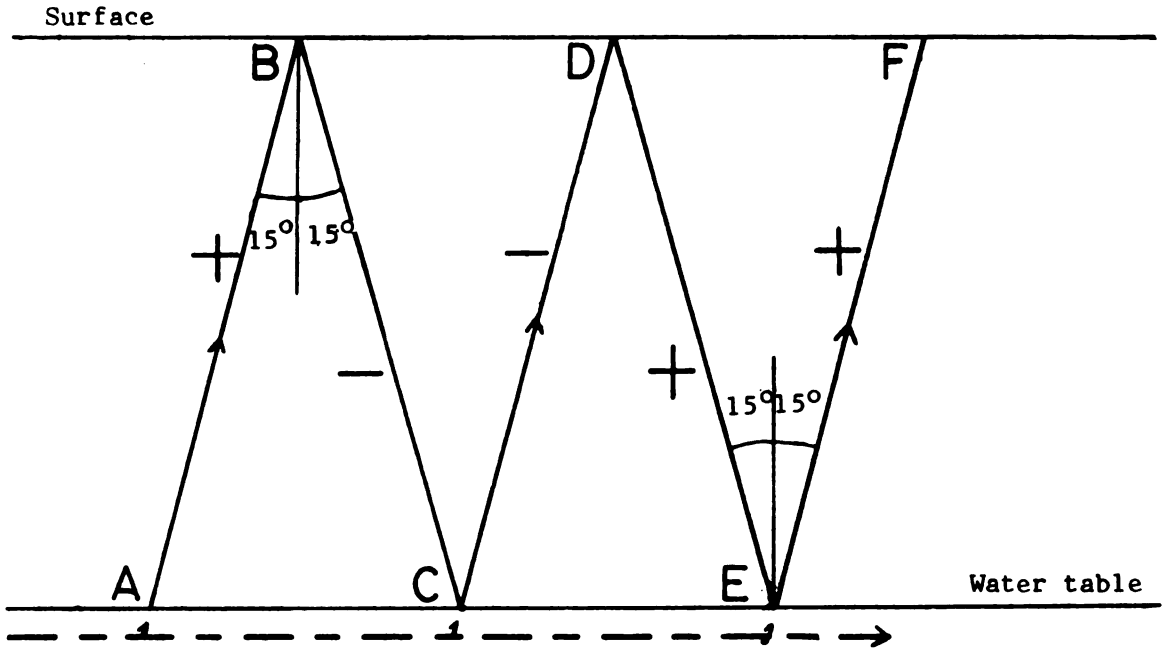

Figure 22.--Travel paths of a multiply reflected refraction arrival.

Thus the third arrival has the same phase as the first, and the second is reversed with respect to the other two. This argument can clearly be extended to any number of pulses. Thus the first, third, fifth, seventh, ninth, etc. pulses are expected to have one phase, and the second, fourth, sixth, eighth, etc. have the opposite phase.

Figure 23 shows arrivals received in just such a manner. The seismic signals are from eight vertical geophones placed twenty-five feet apart at Site One. The closest geophone is 900 feet from the shotpoint. Pulses alternating in phase can be identified for at least eight reversals. In the figure, the received pulses have been marked accordingly with plus and minus signs on the first and eighth traces.

The thickness of the unsaturated layer (i.e., the depth to the water table) has been calculated from the pulses of Figure 23 as a means of verifying the above hypothesis. The average time between pulses of opposite phase is 56 milliseconds. This is the difference in travel time between a path such as CDEF and CEF in the preceding diagram. The EF segment is common to both paths, so that the time difference is that between path CDE at 1150 ft/sec and path CE at 5700 ft/sec. The two travel times can be calculated from the velocities and the geometric relationships. They are expressed as follows:

$$t_{CDE} = \frac{2\ Z}{\cos\ 15^\circ}\ \frac{1}{1150} \qquad t_{CE} = \frac{2\ Z\ \tan\ 15^\circ}{5700}.$$

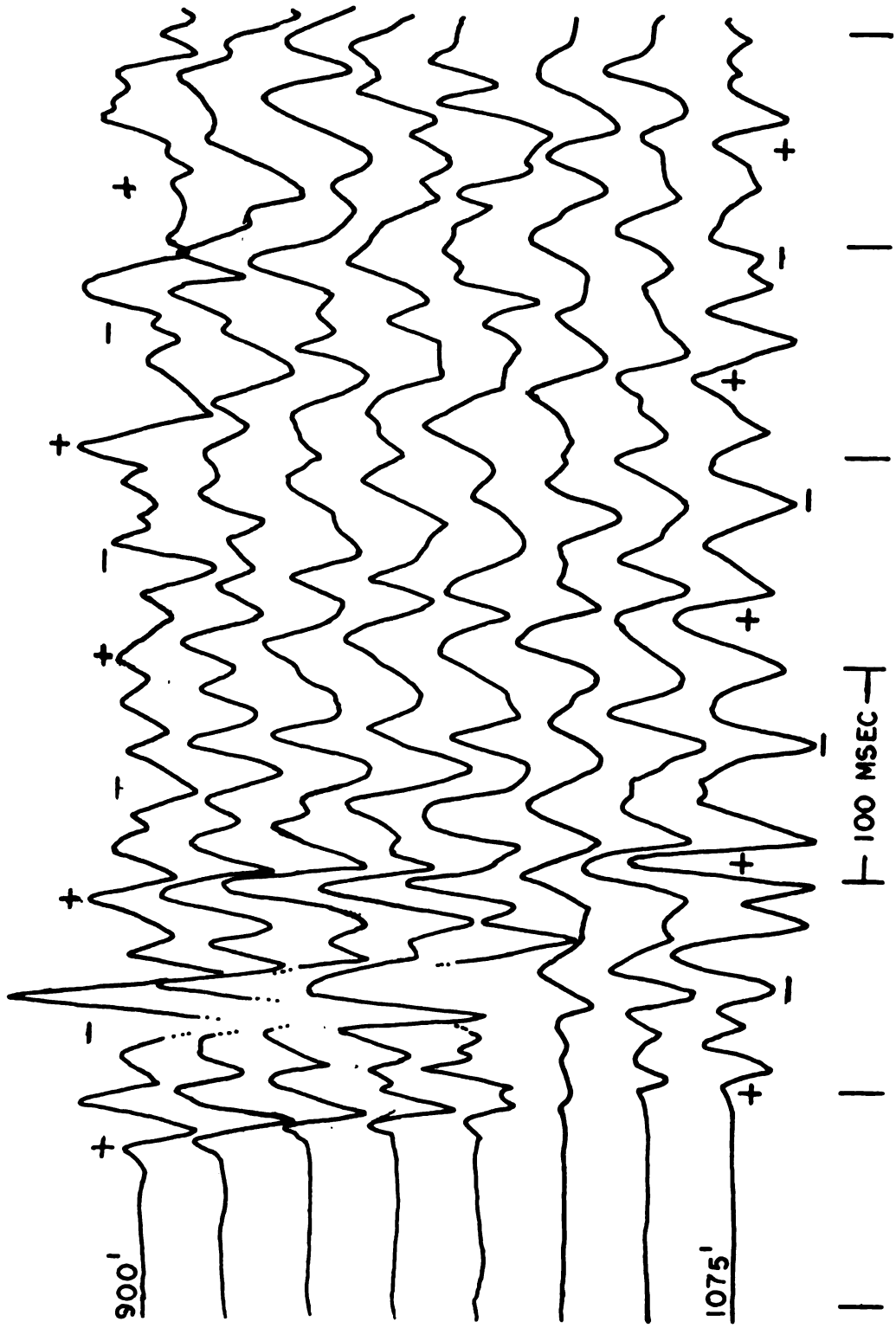

Figure 23.--The multiply reflected refraction arrival at eight vertical geophones.

The depth Z can be found by equating the difference in the travel times of the two segments, 0.00171 Z, with the observed difference of 56 milliseconds. The calculated depth is 33 feet. This figure agrees closely with the 32 feet measured at a nearby test well, and the agreement tends to confirm the hypothesis.

CHAPTER VIII

CONCLUSIONS

This study has shown that three-component recording can provide information about a surface layer that would be missed in conventional vertical recording. A more accurate compressional velocity determination in the surface layer and the discovery of a surface wave related to the direct arrival resulted from analysis of the three-component data.

Plots of the magnitude of particle velocity without reference to direction have been shown to be useful in the interpretation of three-component seismic signals. The method is new and is potentially valuable in recognising some seismic arrivals that might otherwise be overlooked.

The surface wave discovered through the use of this method apparently has not been reported in the literature. Its propagation is linked to the wave guide properties of a relatively thin surface layer with a low velocity relative to the underlying material. It is identified on an observational basis by its elliptical particle motion and its arrival time. It can be predicted at least in a qualitative sense from the theory of seismic ray propagation.

Some aspects of seismic theory related to phase changes upon reflection have been experimentally confirmed. A phase reversal occurs with reflection from a free surface and no phase change occurs with reflection from an interface with material having a higher acoustic impedance.

Suggestions for Further Work

The method of plotting absolute magnitudes of particle velocity as a function of time should be applied to other locations, where it may be able to enhance other seismic signals which are normally ignored in recording and interpretation.

The relationship between the physical properties of the surface layer and the observable characteristics of the surface wave related to the direct arrival--such as frequency spectrum, dispersion, and amplitude ratios--has not been investigated. It should be possible to deduce some of the physical properties of the surface material and its interface with the underlying material from the characteristics of the surface waves.

Surface waves of the type shown to exist have not been evaluated on a rigid theoretical basis. This will not be a simple task, because the reflections and conversions from a solid-state interface require the use of the Zoeppritz equations to evaluate phase changes and the

partition of energy into each of the possible emergent waves. The ground mation must be treated as the sum of compressional and shear motions.

LIST OF REFERENCES

LIST OF REFERENCES

Bennett, H. F. 1970. Personal Communication.

Control Data Corporation. 1965. 3400/3600/3800 computer systems Fortran reference manual. Minneapolis: Control Data Corporation.

Dobrin, M. B., Simon, R. F., and Lawrence, P. L. 1951. "Rayleigh waves from small explosions." Transactions, American Geophysical Union, XXXII, 822-832.

Dobrin, M. B., Lawrence, P. L., and Sengbush, R. L. 1954. "Surface and near-surface waves in the Delaware Basin." Geophysics, IV, 695-715.

Dobrin, M. B. 1960. Introduction to Geophysical Prospecting. New York: McGraw-Hill Book Co., Inc.

Geo Space Corporation. 1965. Frequency response curves for HS-1 geophone. Catalog Sheet.

Harris, M. H., and Gardner, G. H. 1968. Velocity and attenuation of elastic waves in sand. Pittsburg: Gulf Research and Development Co., Technical Memorandum.

Jakosky, J. J. 1950. Exploration Geophysics. Newport Beach, Calif.: Trija Publishing Co.

Jolly, R. N. 1956. "Investigation of Shear Waves." Geophysics, IV, 905-938.

Officer, C. B. 1958. Introduction to the Theory of Sound Transmission. New York: McGraw-Hill Book Company, Inc.

Richter, C. F. 1958. Elementary Seismology. San Francisco: W. H. Freeman and Company.

Shimshoni, Michael, and Smith, S. W. 1964. "Seismic signal enhancement with three component detectors." Geophysics, XXIX, 664-671.

United States Geological Survey. 1957. Freesoil Quadrangle, Michigan. Fifteen minute series topographic map.

White, J. E., Heaps, S. N., and Lawrence, P. L. "Seismic waves from a horizontal source." Geophysics, XXI, 715-723.

White, J. E. 1964. "Motion product seismograms." Geophysics, XXIX, 288-298.

APPENDIX

APPENDIX

Operation of Digitiser

The procedure used in digitising the seismic records used in this study will be described. The procedure can be divided into the tasks of setting up the record, recording reference information, and actually digitising the data.

The record was set up so that its time axis was parallel to the X-axis of the reading table. The position of the record was adjusted with the aid of the digitiser's visual readout so that the Y-coordinates of a dead trace (i.e., a straight line) were identical on both ends of the record. Then the record was taped to the reading table to keep it in the same position.

The reference information required for each trace is the X value of the time break and the Y value of the zero signal level. These values were recorded by punching first the coordinates of the time break and then punching the coordinates of a point on an undisturbed portion of the trace. The Y-coordinate of the time break and the X-coordinate of the undisturbed point were included in the punched coordinates, but were ignored in later processing. The coordinates of the two points took up the first sixteen

columns of the card, and the remainder of the card was available for manually punched information to identify the trace.

After the reference information had been recorded for a particular trace, the trace was digitised. A new card was fed into the keypunch so that the digital data would begin on the first column of the card. The trace was digitised by slowly moving the reading pencil, a disk of transparent plastic, along the trace. A pair of crosshairs in the pencil allowed its position to be clearly seen in relation to the trace. The footpedal of the digitiser was kept depressed so that a series of points was recorded. The keypunch, set for automatic feed, supplied new cards as needed. Following the last card which contained information for the trace, a card containing "99999999" in the first eight columns was added. This card indicated to the processing computer that the data for the trace had ended.

The Playback Program

The purpose of the Playback program has been explained in the text, and a flow chart of a portion of it shown. The input and output decks of the program will be described in the following, and the program itself listed.

The input deck is shown in Figure A-1. The variable names used there are explained in the input code given in Figure A-2. The data is read from the cards according to

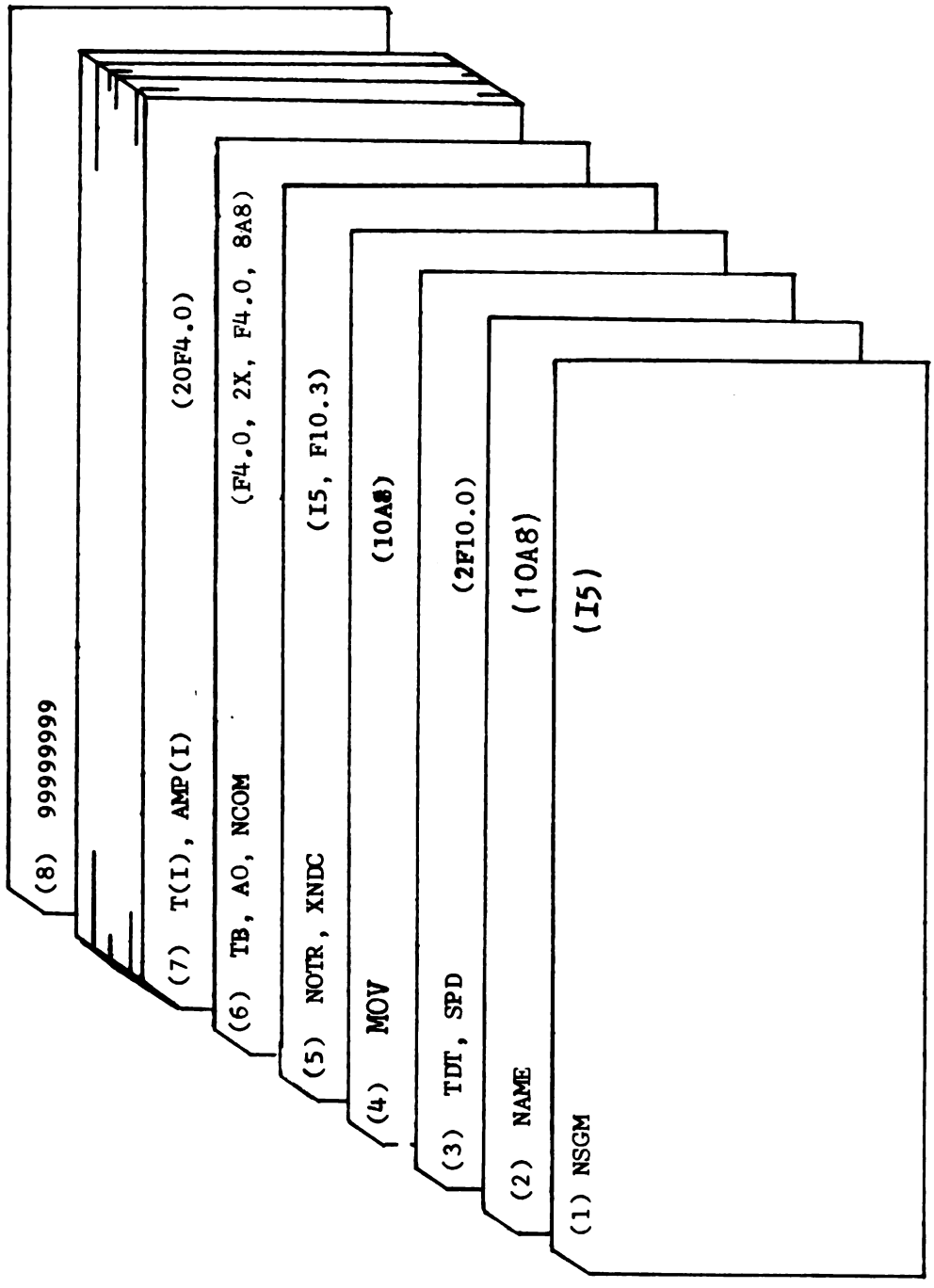

Figure A-1.--Input deck for Playback program.

NSGM: Number of seismic records to be processed.

NAME: Seismic record identification.

TDT: Maximum record time of the digitized portion of the seismogram, in second.

SPD: Camera film speed, in inches/sec.

MØV: Movement identification (e.g.: X, Y, Z, or HL, HT, V)

NØTR: Trace number.

XNDC: Amplification gain.
If XNDC = 0, the trace is dead and cards 6-8 for this trace are not submitted. To reverse polarity, negative values are used.

TB: Time break X-value.

AO: Zero amplitude value.

NCØM: Any comments needed.

T: Signal X-value.

Figure A-2.--Input code for the Playback program.

the FORMAT specifications shown (Control Data Corporation, 1965, p. 9-1).

The function of the cards of Figure A-1 are as follows:

Card 1: The number of seismograms to be processed. If more than one, then another Card 2 will follow the last card of the first seismogram.

Card 2: The name of the seismogram. Whatever data is punched on this card is repeated on all printed, punched, or plotted output for identification.

Card 3: The digitised length of the seismogram in seconds.

Card 4: The name of the direction of movement represented by the following eight traces.

Card 5: The first card for a particular trace. It gives the number of the trace (1 through 24) and the XNDC indicator. This indicator has been mentioned previously as a multiplying factor. In addition, if it is zero or blank, it indicates that there is no data for the particular trace, and that the next card is another Card 5 for the following trace.

Card 6: This is the card containing reference data as described above. It has the time break X value, the zero signal Y value, and identifying information.

Card 7: The digitiser output card. In contrast to the preceding cards, this one has been punched completely

under control of the digitiser. It appears as many times as necessary to transmit the data for the whole trace. The first four characters give the X-coordinate of a point on the trace, in units of tenths of millimeters. The following four characters give the Y-coordinates of the same point. These constitute an eight-column field which is repeated nine times to give the coordinates of ten points on the trace.

Card 8: The last card for a particular trace. The "99999999" in the first eight indicates that all the data for the trace has been transmitted. The next card is a Card 5 unless the "99999999" card appears with the data for the eighth or sixteenth trace. In that case, all the data for a movement direction has been given, and the next card is a Card 4 to identify a new direction of movement. Appearing with a twenty-fourth trace, the "99999999" card is the last card of the seismogram. The statements about this card for the eighth, sixteenth, or twenty-fourth traces also apply to a Card 5 for those traces if the Card 5 contains a zero XNDC indicator.

The input data described above is used by the computer to generate a plotted seismogram of the digitised data and an output deck representing the original data changed and corrected as described in the main text. A description of the output deck follows (see Figure A-3).

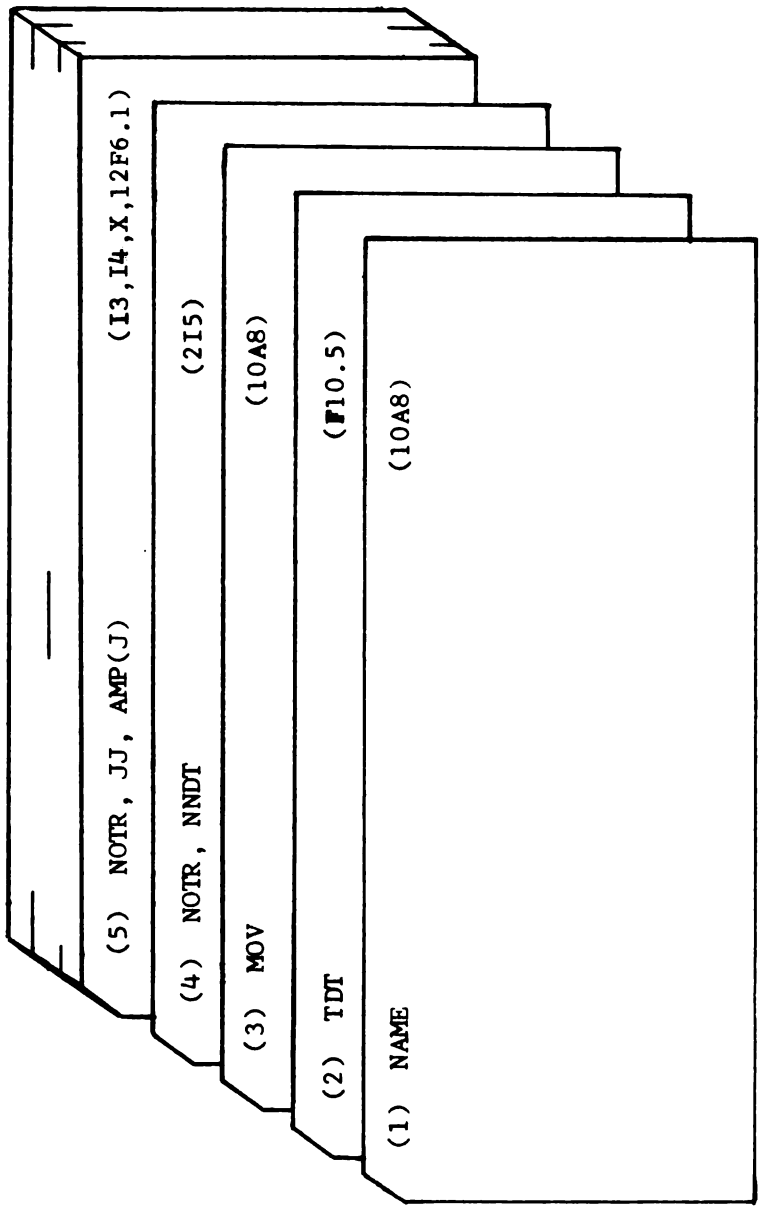

Figure A-3.--Output deck from Playback program.

The order and significance of the data on the output cards will be described with reference to Figure A-3. The names of the variables are explained in the output code given in Figure A-4.

The information given by the punch cards of the output is listed below.

Card 1: The name of the record. This is the same information that appeared on Card 2 of the input deck.

Card 2: The digitised length of the record in seconds.

Card 3: The names of the directions of movement, repeated from the input deck. This card appears three times, separated by the appropriate data.

Card 4: The first card for a particular trace. The number of the trace is given (NOTR), and also the number of data points generated for the trace (NNDT). If NNDT is zero, no data follows, and the next card is another Card 4 or a Card 3.

Card 5: The processed seismic data. The number of the trace is given (NOTR) and also a sequencing number (JJ) to show the position of the card in the deck. No time information is needed because the data points are regularly spaced at 3.3 millisecond intervals. Accordingly, this card carries twelve amplitude values (AMP(J)). Subsequent appearances of this card carry additional groups of twelve amplitude values until all amplitude values for the trace

have been given in order. The sequence number JJ starts at one and advances by one with each new card until the last card for the particular trace. The number of data points given is identical to the number given in Card 4 as NNDT. Following the last appearance of Card 5 is a Card 4 to identify the data of another trace with three exceptions. If the Card 5 was given for the eighth or sixteenth traces, then it is followed by a Card 3. However, the last appearance of Card 5 for the twenty-fourth trace is the last card for the seismogram.

The Absolute Signal Magnitude Program

The absolute signal magnitudes are calculated by a program named SMOV, which used the punched data described above as input. The only change is the addition at the beginning of the deck of a card which specifies the number of input decks to be read (I5 format). The functions of the SMOV program are much more straight-forward than those of the Playback program, and have been adequately described in the main text. The principal output is a computer-drawn plot whose interpretation is also described in the main text. However, some other plots are also drawn but have not been discussed because they are not used in this study. These plots show the absolute signal magnitudes projected on three mutually perpendicular planes.

The computer programs are listed in the following tables. The Playback program is shown in Table A-1 and the SMOV program in Table A-2.

TABLE A-1.--The Playback program.

```
*FTN,X,L,*,R
      PROGRAM PLYBCK
      DIMENSION T(8,1100), NAME(10), XNDC(8),NOPT(8),NOTR(8),MOV(10)
      DIMENSION NNDT(8), NCOM(8),AA(1100),TT(1100)
      COMMON AMP (8, 1100)
    1 FORMAT (*1*)
    2 FORMAT (/)
    3 FORMAT (/,/)
    4 FORMAT (/,/,/)
    5 FORMAT (* SEISMIC DATA PLAY-BACK SYSTEM*)
    6 FORMAT (10A8)
    7 FORMAT (* TRACE NUMBER*, I5, * IS DEAD*)
    8 FORMAT (20F4.0)
    9 FORMAT (I5, F10.3)
   10 FORMAT (F4.0, 8X, F4.0, 8A8 )
   11 FORMAT (X,16F7.1)
   12 FORMAT (2X,8(6X,I2,6X))
   13 FORMAT (* PROGRAM COMPLETED*)
   14 FORMAT (I3,I4,X,12F6.1)
   15 FORMAT (5X, 8A8)
   16 FORMAT  (2I5)
   17 FORMAT  (X, 9F10.3)
   18 FORMAT (2F10.0)
   19 FORMAT (5X,* TIME*, 2X, 8(5X,I2,3X))
   20 FORMAT (I5)
   21 FORMAT (2I5)
   22 FORMAT (F10.5)
C      *****   MAIN PROGRAM    *****
      PRINT 1
      PRINT 4
      PRINT 5
      PRINT 4
C      *****   READING INPUT DATA    *****
C      *****      INPUT CODE      *****
C              NSGM = NUMBER OF SEISMOGRAMS TO BE PROCESSED
```

TABLE A-1.--Continued

```
C               NAME = DATA IDENTIFICATION
C               TDT = AMMOUNT DIGITIZED, IN SECONDS
C               SPD = FILM SPEED, IN INCHES/SECOND
C               MOV = MOVEMENT IDENTIFICATION
C               XNDC = TRACE GAIN, IF XNDC = 0.0, TRACE IS DEAD
C               NOTR = TRACE NUMBER
C               TB = TIME BREAK
C               A0 = ZERO AMPLITUDE
C               NCOM = COMMENT
C               A = AMPLITUDE
C               T = TIME
      DO 20 I = 1, 1100
   20 TT(I) = (I-1)*3.3
      READ 20, NSGM                                                    READ
      PAPER = NSGM*50.00
      CALL PLOT (PAPER, 0.00, 3, 100.0, 100.0)
      DO 56 NRCD = 1, NSGM
      READ 6, NAME                                                     READ
      PRINT 6, NAME
      PUNCH 6, NAME
      READ 18, TDT, SPD                                                READ
      PUNCH 22, TDT
      TCNST = 12.00000/SPD
      PRINT 4
C     *****   AXES SET UP   *****
      CALL PLOT (0.0, 0.0, 2, 100.0, 100.0)
      CALL PLOT (0.0, -30.0, 2)
      CALL AXES (TDT)
      DO 55 NOSTR = 1, 3
      READ 6, MOV                                                      READ
      PRINT 6, MOV
      PUNCH 6, MOV
      PRINT 3
      DO 40 NOTM = 1, 8
      READ 9, NOTR(NOTM), XNDC(NOTM)                                   READ
```

TABLE A-1.--Continued

```
      IF (ABS(XNDC(NOTM)) .LE. 0.0000) GO TO 38
      READ 10, TB, A0, NCOM                                              READ
      PRINT 15, NCOM
      N = 1
      M = 10
   30 READ 8, (T(NOTM,I), AMP(NOTM,I), I = N, M)                         READ
C     *****   IF THE FIRST AMPLITUDE ON THIS CARD IS GREATER THAN
C    1 9000.0, THEN THE PREVIOUS CARD WAS THE LAST CARD FOR THIS TRACE
      IF (AMP(NOTM,N) .GT. 9900) GO TO 31
      N = N + 10
      M = M + 10
      GO TO 30
   31 N = N - 10
      M = M - 10
C     *****   LOOP CHECKS FOR LAST DATA VALUE ON CARD     *****
      DO 32 J = N, M
   32 IF (AMP(NOTM,J) .LE. 0.000) GO TO 33
C     *****   NUMBER OF DATA POINTS ON THE TRACE    *****
   33 NODATA = J - 1
      N = NOPT (NOTM) = NODATA + 1
C     *****   DUMMYING IN ZERO AMPLITUDE AFTER THE LAST DATA POINT    ***
      AMP(NOTM,N) = 0.00000
      T(NOTM,N) = T(NOTM,NODATA) + 10.0000 - TB
      M = N + 1
C     *****   SET REMAINING DATA POINT SPACES EQUAL TO ZERO    *****
      DO 34 I = M, 1100
      T(NOTM, I) = 11000.0
   34 AMP (NOTM, I) = 0.000000
C     *****   REMOVE TIME BREAK AND ZERO AMPLITUDE    *****
      IF (ABS(AMP(NOTM,1)-A0) .LT. 50.0)GO TO 36
      IF (ABS(AMP(NOTM,2)-A0) .LT. 50.0) GO TO 36
      IF (ABS(AMP(NOTM,3)-A0) .LT. 50.0) GO TO 36
      A0 = 0.00000
      DO 35  I = 1, 3
   35 A0 = A0 + AMP(NOTM,I)
```

TABLE A-1.--Continued

```
      AO = AO/3.00000
   36 DO 37 I = 1, NODATA
      AMP (NOTM, I) = (AMP (NOTM, I) - AO) * XNDC(NOTM)
   37 T(NOTM,I) = (T(NOTM,I) - TB)*TCNST
      GO TO 40
C     ***** DUMMY IN ZEROS FOR DEAD TRACES    *****
   38 DO 39 I = 1, 1100
      T(NOTM, I) = 0.000000
   39 AMP(NOTM, I) = 0.000000000
      PRINT 7, NOTR(NOTM)
      NOPT (NOTM) = 0
   40 CONTINUE
C     *****   PRINT OUT INPUT DATA    *****
      PRINT 1
      PRINT 12, (NOTR(I), I = 1, 8)
      PRINT 2
      NODATA = NOPT (1)
      DO 41 I = 2, 8
   41 IF (NODATA .LT. NOPT(I)) NODATA = NOPT(I)
      IF (NODATA .LE. 0) NODATA = 1
      DO 42 J = 1, NODATA
   42 PRINT 11, (T(I,J), AMP(I, J), I = 1, 8)
      PRINT 4
      DO 51 NOX = 1, 8
      TB = 0.00000000
      AB = 0.000000000
      TST = -10.00000
      EOG = 2.00000000
      J = 1
      IF (XNDC(NOX) .LE. 0.000000) GO TO 51
```

TABLE A-1.--Continued

```
      DO 43 I = 1, 1100
   43 AA(I) = AMP(NOX, I)
      EDG = 150.00
      I = 0
C     *****   TIME CHECK AND CORRECT   *****
C      *****   USING A LINEAR APPROXIMATION BETWEEN CONTROL POINTS  ****
   44 I = I + 1
      IF (I .GE. 1100) GO TO 51
      IF (T(NOX,I) .GE. 11000.0) GO TO 48
      IF (T(NOX,I) .LE. TB) GO TO 44
      IF (ABS(AA(I)-AB) .GT.EDG) GO TO 44
      TST = TST + 10.000000
   45 IF (ABS(T(NOX,I)-TST) .GT. EDG) GO TO 46
      TB = TST
      AMP (NOX,J) = AB = AA(I)
      J = J + 1
      GO TO 44
   46 IF (T(NOX,I) .GT. TST) GO TO 47
      TB = T(NOX,I)
      AB = AA(I)
      GO TO 48
   47 SLP = (AA(I) - AB)/(T(NOX,I) - TB)
      AMP (NOX, J) = AB + SLP*( TST - TB)
      AB = AMP (NOX,J)
      TB = TST
      J = J + 1
      TST = TST + 10.0
      GO TO 45
   48 I = I + 1
      IF (I .GE. 1100) GO TO 51
      IF (T(NOX,I) .GE. 11000.0) GO TO 48
      IF (T(NOX,I) .LE. TB) GO TO 48
      IF (ABS(AA(I)-AB) .GT.EDG) GO TO 48
```

TABLE A-1.--Continued

```
      GO TO 45
   49 DO 50 I = J, 1100
   50 AMP (NOX,I) = 0.000000000
   51 NNDT(NOX) = J - 1
C     *****   PRINTING OUT CORRECTED DATA    *****
      PRINT 1
      PRINT 6, MOV
      PRINT 3
      PRINT 10, (NOTR(I), I = 1, 8)
      PRINT 2
      NODATA = NNDT(1)
      DO 52 I = 2, 8
   52 IF (NODATA .LT. NNDT(I)) NODATA = NNDT(I)
      IF (NODATA .LE. 0) NODATA = 1
      DO 53 J = 1, NODATA
      N = J/12
      PRINT 17, TT(J), (AMP(I,J), I = 1, 8)
   53 IF (12*N .EQ. J) PRINT 2
C     *****   PLOTTING CORRECTED  DATA    *****
      CALL DATPLT(NODATA)
      CALL PLOT (0.00, 0.00, 0, 100.0, 100.0)
      CALL PLOT (0.5, -1.5, 3)
      CALL CHAR (0.5, -1.5, MOV, 80, 90.0, 0.25, 0.15, 0.5)
      CALL PLOT (0.00, 0.00, 3)
      DO 55 I = 1, 8
      PUNCH 21, NOTR(I), NNDT(I)
      IF (NNDT(I) .EQ. 0) GO TO 55
      JJ = 0
      JND = 0
   54 JST = JND + 1
      IF (JST .GT. NNDT(I)) GO TO 55
      JJ = JJ + 1
      JND = JST + 11
```

TABLE A-1.--Continued

```
      PUNCH 14, NOTR(I), JJ, (AMP(I,J), J = JST, JND)
      GO TO 54
   55 CONTINUE
      CALL PLOT (0.00, 0.00, 0, 100.0, 100.0)
      CALL CHAR (0.00, 0.0,NAME, 80, 90.0, 0.25, 0.15, 0.5)
      CALL PLOT (0.0, 2.0, 2)
      CALL CHAR (0.0, 2.0, 9HPLAY-BACK, 9, 90.0, 0.5, 0.3, 0.5)
      FIN = 12*TDT + 10.0
      CALL PLOT (FIN, 0.0, 2)
   56 CONTINUE
      CALL PLOT (FIN,0.0,-1)
      PRINT 1
      PRINT 13
      END
```

TABLE A-1.--Continued

```
      SUBROUTINE AXES (TDT)
C     *****   TIME AXES SET-UP   *****
      CALL PLOT (0.0, 0.0, 0, 100.0, 100.0)
      NSD = TDT
      IF (NSD .LT. TDT) NSD = NSD + 1
C     TOP = UPPER MARGIN SPACE + 0.05 INCH
C     FOR EXAMPLE, IF U M  = 6.0 IN, AND SPACE = 2.5, THEN TOP = 3.45, OR..
      X = 3.45
      DO 13 NM = 1, 3
C     NOGR = NUMBER OF B-TRACE GROUPS
C     FOR EXAMPLE, IF NOGR = 3, THEN....
      X = X + 2.50
      T = 0.12
      CALL PLOT (T, X, 2)
      DO 6 NS = 1, NSD
      DO 5 NT = 1, 10
      DO 1 NH = 1, 2
      X = X + 0.10
      CALL PLOT (T, X, 1)
      T = T + 0.12
      CALL PLOT (T, X, 2)
      X = X - 0.10
      CALL PLOT (T, X, 1)
      T = T + 0.12
    1 CALL PLOT (T, X, 2)
      X = X - 0.05
      CALL PLOT (T, X, 2)
      X = X + 0.20
      CALL PLOT (T, X, 1)
      X = X - 0.05
      T = T + 0.12
      CALL PLOT (T, X, 2)
      DO 2 NH = 1, 2
```

TABLE A-1.--Continued

```
      X = X - 0.10
      CALL PLOT (T, X, 1)
      T = T + 0.12
      CALL PLOT (T, X, 2)
      X = X + 0.10
      CALL PLOT (T, X, 1)
      T = T + 0.12
    2 CALL PLOT (T, X, 2)
      IF (NT .GE. 10) GO TO 5
      IF (NT .EQ. 5) GO TO 3
      X = X + 0.20
      CALL PLOT  (T, X, 2)
      X = X - 0.50
      CALL PLOT (T, X, 1)
      X = X + 0.20
      GO TO 4
    3 X = X + 0.45
      CALL PLOT (T, X, 2)
      X = X - 1.00
      CALL PLOT (T, X, 1)
      X = X + 0.45
    4 T = T + 0.12
    5 CALL PLOT (T, X, 2)
      X = X + 0.95
      CALL PLOT (T, X, 2)
      X = X - 2.00
      CALL PLOT (T, X, 1)
      X = X + 0.95
      T = T + 0.12
    6 CALL PLOT (T, X, 2)
      X = X + 3.50
      T = T - 0.12
      DO 12 NS = 1, NSD
      X = X - 0.95
      CALL PLOT (T, X, 2)
```

TABLE A-1.--Continued

```
      X = X + 2.00
      CALL PLOT (T, X, 1)
      X = X - 0.95
      T = T - 0.12
      CALL PLOT  (T, X, 2)
      DO 11 NT = 1, 10
      DO 7 NH = 1, 2
      X = X - 0.10
      CALL PLOT (T, X, 1)
      T = T - 0.12
      CALL PLOT (T, X, 2)
      X = X + 0.10
      CALL PLOT (T, X, 1)
      T = T - 0.12
    7 CALL PLOT (T, X, 2)
      X = X + 0.05
      CALL PLOT (T, X, 2)
      X = X - 0.20
      CALL PLOT (T, X, 1)
      X = X + 0.05
      T = T - 0.12
      CALL PLOT (T, X, 2)
      DO 8 NH = 1, 2
      X = X + 0.10
      CALL PLOT (T, X, 1)
      T = T - 0.12
      CALL PLOT (T, X, 2)
      X = X - 0.10
      CALL PLOT (T, X, 1)
```

TABLE A-1.--Continued

```
      T = T - 0.12
    8 CALL PLOT (T, X, 2)
      IF (NT .GE. 10) GO TO 11
      IF (NT .EQ. 5) GO TO 9
      X = X - 0.20
      CALL PLOT (T, X, 2)
      X = X + 0.50
      CALL PLOT (T, X, 1)
      X = X - 0.20
      GO TO 10
    9 X = X - 0.45
      CALL PLOT (T, X, 2)
      X = X + 1.00
      CALL PLOT (T, X, 1)
      X = X - 0.45
   10 T = T - 0.12
   11 CALL PLOT (T, X, 2)
   12 CONTINUE
   13 CONTINUE
      CALL PLOT (0.00, 23.50, 2)
      CALL PLOT (0.00, 4.00, 1)
C     IF U M   = 6.0 IN. THEN ....
      CALL PLOT (0.00, 6.00, 2)
      RETURN
      END
```

TABLE A-1.--Continued

```
      SUBROUTINE DATPLT (NDT)
C     PLOTS 8 TRACES OF DATA PER GROUP ON AXES
      COMMON AMP (8, 1100)
      DIMENSION T(1100)
      DO 1 I = 1, 1100
    1 T(I) = (I-1)*10.00
      J = 0
      DO 4 NX = 1, 4
      CALL PLOT (0.00, 0.00, 0, 0.3937, 0.3937)
      J = J + 1
      DO 2 NT = 1, NDT
      X = -AMP(J,NT)
    2 CALL PLOT (T(NT), X, 1)
      CALL PLOT (T(NDT), 127.0, 2)
      J = J + 1
      CALL PLOT (T(NDT), 0.0, 0, 0.3937, 0.3937)
      DO 3 NT = 1, NDT
      NNT = NDT + 1 - NT
      X = -AMP(J,NNT)
    3 CALL PLOT (T(NNT), X, 1)
    4 CALL PLOT (0.0, 127.0, 2)
C     GRSP = ((INTERGROUP SPACING) / 0.3937) 100
C     FOR EXAMPLE, IF I G S  = 2.5 IN, THEN GRSP=(2.5/0.3937)100 = 635.80
      CALL PLOT (0.0, 635.80, 2)
      RETURN
      END
*RUN,1,30,2100,*7,M
```

TABLE A-2.--The SMOV program.

```
!FTN,X,L,*,R,P
      PROGRAM SMOV
      DIMENSION NAME(10), AA(1100), NOTR(3,8), NMV(10), INDC(3,8)
      DIMENSION AL(10), AV(10), AT(10), NPT(5), I(1100)
      COMMON AMP(8,1100)
    1 FORMAT (*1*)
    2 FORMAT (/)
    3 FORMAT (/,/)
    4 FORMAT (/,/,/)
    5 FORMAT (* GROUND MOTION STUDY*)
    6 FORMAT (10A8)
    7 FORMAT (8X, 12F6.1)
    8 FORMAT (2I5, F10.5)
    9 FORMAT (* TRACE NUMBER*, I5, *  IS DEAD*)
   10 FORMAT (8F10.3)
   11 FORMAT (3X, * TIME*, 8(5X,I2,3X))
   12 FORMAT (* TOTAL ABSOLUTE MOTIONS*)
   13 FORMAT (* XZ MOTIONS*)
   14 FORMAT (* YZ MOTIONS*)
   15 FORMAT (* XY MOTIONS*)
   16 FORMAT (* PROGRAM COMPLETED*)
   17 FORMAT (F10.0)
   18 FORMAT (I5)
C       *****   MAIN PROGRAM    *****
      PRINT 1
      PRINT 4
      PRINT 5
      PRINT 3
C     *****   READING INPUT    *****
C     *****   INPUT CODE    *****
C             NOSGM = NUMBER OF SEISMIC RECORDS TO BE PROCESSED
C             NAME = DATA IDENTIFICATION
C             NMV = MOVEMENT IDENTIFICATION
```

TABLE A-2.--Continued

```
C               NOTR = TRACE NUMBER
C               INDC = NUMBER OF DATA POINTS ON TRACE
C               GN = AMPLITUDE GAIN INDICATOR, GAIN = 1, FOR GN = 0
C               AMP = AMPLITUDE
      READ 18, NOSGM
      PAPER = 50*NOSGM
      CALL PLOT (PAPER, 0.00, 3, 100.0, 100.0)
      DO 46 NORCD = 1, NOSGM
      READ 6, NAME                                                    READ
      PRINT 6, NAME
      READ 17, TDT
C     *****    AXES SET-UP    *****
       CALL PLOT (0.0,0.0, 0, 100.0, 100.0)
      CALL PLOT (0.0, -30.0, 2)
      CALL AXES (TDT)
      PRINT 3
      DO 29 I = 1, 1100
   29 T(I) = 3.3*I
      DO 37 NOMV = 1, 3
      READ 6, NMV                                                     READ
      PRINT 6, NMV
      PRINT 3
      DO 34 NOPH = 1, 8
      GAIN = 1.000000
      READ 8,(NOTR(NOMV, NOPH), INDC(NOMV,NOPH), GN)
      IF (ABS(GN) .GT. 0.000001) GAIN = GN
      PRINT 8, (NOTR(NOMV,NOPH), INDC(NOMV,NOPH), GAIN)
      IF (INDC(NOMV,NOPH) .EQ. 0) GO TO 32
      NND = INDC(NOMV,NOPH)
      READ 7, (AMP(NOPH,I), I = 1, NND)                               READ
      DO 30 I = 1, NND
   30 AMP(NOPH,I) = GAIN*AMP(NOPH,I)
      NND = NND + 1
```

TABLE A-2.--Continued

```
      DO 31 I = NND,1100
   31 AMP(NOPH,I) = 0.000000
      GO TO 34
   32 PRINT 9, NOTR(NOMV,NOPH)
      PRINT 3
      DO 33 I = 1,1100
   33 AMP(NOPH,I) = 0.000000000
   34 CONTINUE
      NODATA = INDC(NOMV,1)
      DO 35 I = 2, 8
   35 IF (NODATA .LT. INDC(NOMV,I)) NODATA = INDC(NOMV,I)
      IF (NODATA .LE. 0) NODATA = 1
      NPT(NOMV) = NODATA
C     *****   STORING DATA ON STORAGE DRUM   *****
      NODM = 20 + NOMV
      REWIND NODM
      DO 36 J = 1,1100
   36 WRITE (NODM), (AMP(I,J), I = 1, 8)
      REWIND NODM
C     *****   PRINTING OUT INPUT DATA   *****
      PRINT 11, (NOTR(NOMV, I), I = 1,8)
      PRINT 2
      PRINT 10, (T(J), (AMP(I,J), I = 1, 8), J = 1, NODATA)
   37 PRINT 4
C     *****   GROUND MOTION AMPLITUDE   *****
C     *****   TOTAL AMPLITUDE   *****
      PRINT 1
      PRINT 4
      PRINT 12
      PRINT 2
      NODATA = MAX0(NPT(1),NPT(2),NPT(3))
      IF (NODATA .LE. 0) NODATA = 1
      DO 38 I = 1, 3
```

TABLE A-2.--Continued

```
      DO 38 J = 1, 8
   38 IF (INDC(I,J) .EQ. 0) PRINT 9, J
      DO 39 NOTM = 1, NODATA
      READ (21), (AL(I), I = 1, 8)
      READ (22),  (AV(I), I = 1, 8)
      READ (23), (AT(I), I = 1,8)
      DO 39 I = 1, 8
      AMP(I,NOTM) = SQRT(AL(I)**2 + AV(I)**2 + AT(I)**2)
      DO 39 J = 1, 3
   39 IF (NOTM .GT. INDC(J,I)) AMP(I,NOTM) = 0.00000
      PRINT 4
      PRINT 11, (I, I = 1, 8)
      PRINT 2
      PRINT 10, (T(J), (AMP(I,J), I = 1,8), J = 1, NODATA)
      REWIND 21
      REWIND 22
      REWIND 23
      CALL DATPLT (NODATA)
      CALL PLOT (0.00, 0.00, 0, 100.0, 100.0)
      CALL PLOT (0.5, -1.0, 2)
      CALL CHAR (0.5, -1.0, 15HTOTAL AMPLITUDE, 15, 90.0, 0.25, 0.15,
     1 0.5)
      CALL PLOT (0.00, 0.00, 2)
C     *****   X-Z MOTION   *****
      PRINT 1
      PRINT 4
      PRINT 13
      PRINT 2
      NDT = MAX0 (NPT(1),NPT(2))
      IF (NDT .LE. 0) NDT = 1
      DO 40 I = 1, 2
      DO 40 J = 1, 8
   40 IF (INDC(I,J) .EQ. 0) PRINT 9, J
      DO 41 NOTM = 1, NDT
      READ (21), (AL(I), I = 1,8)
      READ (22), (AV(I), I = 1,8)
```

TABLE A-2.--Continued

```
      DO 41 I = 1, 8
      AMP(I,NOTM) = SQRT(AL(I)**2 + AV(I)**2)
      DO 41 J = 1, 2
   41 IF (NOTM .GT. INDC(J,I)) AMP(I,NOTM) = 0.000000
      PRINT 4
      PRINT 11, (I, I = 1, 8)
      PRINT 2
      PRINT 10, (T(J), (AMP(I,J), I = 1,8), J = 1, NDT)
      REWIND 21
      REWIND 22
      CALL DATPLT (NDT)
      CALL PLOT (0.00, 0.00, 0, 100.0, 100.0)
      CALL PLOT (0.5, -1.0, 2)
      CALL CHAR (0.5, -1.0, 10HX-Z MOTION, 10, 90.0, 0.25, 0.15, 0.5)
      CALL PLOT (0.00, 0.00, 2)
C     *****   Y-Z MOTION   *****
      PRINT 1
      PRINT 4
      PRINT 14
      PRINT 2
      NDT = MAX0(NPT(2),NPT(3))
      IF (NDT .LE. 0) NDT = 1
      DO 42 I = 2, 3
      DO 42 J = 1, 8
   42 IF (INDC(I,J) .EQ. 0) PRINT 9, J
      DO 43 NOTM = 1, NDT
      READ (22), (AV(I), I = 1,8)
      READ (23) (AT(I), I = 1,8)
      DO 43 I = 1, 8
      AMP (I,NOTM) = SQRT(AV(I)**2 + AT(I)**2)
      DO 43 J = 2, 3
   43 IF (NOTM .GT. INDC(J,I)) AMP(I,NOTM) = 0.000000
      PRINT 4
```

TABLE A-2.--Continued

```
      PRINT 11, (I, I = 1, 8)
      PRINT 2
      PRINT 10, (T(J), (AMP(I,J), I = 1,8), J = 1 ,NDT)
      REWIND 22
      REWIND 23
      CALL DATPLT (NDT)
      CALL PLOT (0.00, 0.00, 0, 100.0, 100.0)
      CALL PLOT (0.5, -1.0, 2)
      CALL CHAR (0.5, -1.0, 10HY-Z MOTION, 10, 90.0, 0.25, 0.15, 0.5)
      CALL PLOT (0.00, 0.00, 2)
      *****   X-Y MOTION   *****
      PRINT 1
      PRINT  4
      PRINT 15
      PRINT 2
      NDT = MAXO (NPT(1),NPT(3))
      IF (NDT .LE. 0) NDT = 1
      DO 44 I = 1, 8
      IF (INDC(1,I) .EQ. 0) PRINT 9, I
   44 IF (INDC(3,I) .EQ. 0) PRINT 9, I
      DO 45 NOTM = 1, NDT
      READ (21), (AL(I), I = 1, 8)
      READ (23), (AT(I), I = 1,8)
      DO 45 I = 1, 8
      AMP(I,NOTM) = SQRT(AL(I)**2 + AT(I)**2)
      IF (NOTM .GT. INDC(1,I)) AMP(I,NOTM) = 0.000000
   45 IF (NOTM .GT. INDC(3,I)) AMP(I,NOTM) = 0.000000
      PRINT 4
      PRINT 11, (I, I = 1, 8)
      PRINT 2
      PRINT 10, (T(J), (AMP(K,J), K = 1,8), J = 1, NDT)
      CALL DATPLT (NDT)
      CALL PLOT (0.00, 0.00, 0, 100.0, 100.0)
```

TABLE A-2.--Continued

```
      CALL PLOT (0.5, -1.0, 2)
      CALL CHAR (0.5, -1.0, 10HX-Y MOTION, 10, 90.0, 0.25, 0.15, 0.5)
      CALL PLOT (0.00, 0.00, 2)
      CALL PLOT (0.0, 0.0, 0, 100.0, 100.0)
      CALL PLOT (0.5, 0.0, 2)
      CALL CHAR (0.5, 0.0, 4HSMOV, 4, 90.0, 0.5, 0.2, 0.5)
      CALL PLOT (0.5, 2.0, 2)
      CALL CHAR (0.5, 2.0, NAME, 80, 90.0, 0.25, 0.15, 0.5)
      FIN = 12*TDT + 10.0
      CALL PLOT (FIN, 0.0, 2)
   46 CONTINUE
      CALL PLOT (FIN, 0.0, -1)
      PRINT 1
      PRINT 16
      END
```

TABLE A-2.--Continued

```
      SUBROUTINE AXES (TOT)
C     *****   TIME AXES SET-UP   *****
      CALL PLOT (0.0, 0.0, 0, 100.0, 100.0)
      NSD = TOT
      IF (NSD .LT. TOT) NSD = NSD + 1
C     *****   TOP = UPPER MARGIN SPACE - SPACE - 0.05   *****
C     *****   FOR EXAMPLE, IF U.M. = 5.00 IN., AND SPACE = 2.0 IN.,
C    1 THEN, TOP = 2.95 IN. OR,
      X = 2.95
C     *****   DO 13 NM = 1, NOGR   *****
C     *****   NOGR = NUMBER OF 8-TRACE GROUPS   *****
      DO 13 NM = 1, 4
C     *****   FOR EXAMPLE, IF NOGR = 4, THEN   *****
      X = X + 2.00
      T = 0.12
      CALL PLOT (T, X, 3)
      DO 6 NS = 1, NSD
      DO 5 NT = 1, 10
      DO 1 NH = 1, 2
      X = X + 0.10
      CALL PLOT (T, X, 1)
      T = T + 0.12
      CALL PLOT (T, X, 2)
      X = X - 0.10
      CALL PLOT (T, X, 1)
      T = T + 0.12
    1 CALL PLOT (T, X, 2)
      X = X - 0.05
      CALL PLOT (T, X, 2)
      X = X + 0.20
      CALL PLOT (T, X, 1)
      X = X - 0.05
      T = T + 0.12
```

TABLE A-2.--Continued

```
      CALL PLOT (T, X, 2)
      DO 2 NH = 1, 2
      X = X - 0.10
      CALL PLOT (T, X, 1)
      T = T + 0.12
      CALL PLOT (T, X, 2)
      X = X + 0.10
      CALL PLOT (T, X, 1)
      T = T + 0.12
    2 CALL PLOT (T, X, 2)
      IF (NT .GE. 10) GO TO 5
      IF (NT .EQ. 5) GO TO 3
      X = X + 0.20
      CALL PLOT  (T, X, 2)
      X = X - 0.50
      CALL PLOT (T, X, 1)
      X = X + 0.20
      GO TO 4
    3 X = X + 0.45
      CALL PLOT (T, X, 2)
      X = X - 1.00
      CALL PLOT (T, X, 1)
      X = X + 0.45
    4 T = T + 0.12
    5 CALL PLOT (T, X, 2)
      X = X + 0.95
      CALL PLOT (T, X, 2)
      X = X - 2.00
      CALL PLOT (T, X, 1)
      X = X + 0.95
      T = T + 0.12
    6 CALL PLOT (T, X, 2)
      X = X + 3.50
```

TABLE A-2.--Continued

```
      T = T - 0.12
      DO 12 NS = 1, NSD
      X = X - 0.95
      CALL PLOT (T, X, 2)
      X = X + 2.00
      CALL PLOT (T, X, 1)
      X = X - 0.95
      T = T - 0.12
      CALL PLOT  (T, X, 2)
      DO 11 NT = 1, 10
      DO 7 NH = 1, 2
      X = X - 0.10
      CALL PLOT (T, X, 1)
      T = T - 0.12
      CALL PLOT (T, X, 2)
      X = X + 0.10
      CALL PLOT (T, X, 1)
      T = T - 0.12
    7 CALL PLOT (T, X, 2)
      X = X + 0.05
      CALL PLOT (T, X, 2)
      X = X - 0.20
      CALL PLOT (T, X, 1)
      X = X + 0.05
      T = T - 0.12
      CALL PLOT (T, X, 2)
      DO 8 NH = 1, 2
      X = X + 0.10
      CALL PLOT (T, X, 1)
      T = T - 0.12
      CALL PLOT (T, X, 2)
      X = X - 0.10
      CALL PLOT (T, X, 1)
```

TABLE A-2.--Continued

```
      T = T - 0.12
    8 CALL PLOT (T, Y, 2)
      IF (NT .GE. 10) GO TO 11
      IF (NT .EQ. 5) GO TO 9
      X = X - 0.20
      CALL PLOT (T, Y, 2)
      X = X + 0.50
      CALL PLOT (T, Y, 1)
      X = X - 0.20
      GO TO 10
    9 X = X - 0.45
      CALL PLOT (T, Y, 2)
      X = X + 1.00
      X = X - 0.45
      CALL PLOT (T, Y, 1)
   10 T = T - 0.12
   11 CALL PLOT (T, Y, 2)
   12 CONTINUE
   13 CONTINUE
      CALL PLOT (0.00, 27.50, 2)
      CALL PLOT (0.00, 3.50, 1)
C     IF (U M = 5.00 IN.) THEN ....
      CALL PLOT (0.00, 5.00, 2)
      RETURN
      END
```

TABLE A-2.--Continued

```
      SUBROUTINE DATPLT (NDT)
C     PLOTS 8 TRACES OF DATA PER GROUP ON AXES
      COMMON AMP (8, 1100)
      DIMENSION T(1100)
      DO 1 I = 1, 1100
    1 T(I) = (I-1)*10.00
      J = 0
      DO 4 NX = 1, 4
      CALL PLOT (0.00, 0.00, 0, 0.3937, 0.3937)
      J = J + 1
      DO 2 NT = 1, NDT
      X = -AMP(J,NT)
    2 CALL PLOT (T(NT), X, 1)
      CALL PLOT (T(NDT), 127.0, 2)
      J = J + 1
      CALL PLOT (T(NDT), 0.0, 0, 0.3937, 0.3937)
      DO 3 NT = 1, NDT
      NNT = NDT + 1 - NT
      X = -AMP(J,NNT)
    3 CALL PLOT (T(NNT), X, 1)
    4 CALL PLOT (0.0, 127.0, 2)
C     GPSP = ((INTERGROUP SPACING) / 0.3937) 100
C     FOR EXAMPLE, IF I.G.S. = 2.0 IN, THEN GPSP=(2.0/0.3937)100 = 508.00
      CALL PLOT (0.0, 508.00, 2)
      RETURN
      END
```